Georgia Water Resources Institute

Annual Technical Report

FY 2000

Introduction

In Fiscal Year 2000, the Georgia Water Resources Institute (GWRI) was involved in a wide range of activities at the state, national, and international levels.

In summary, the following GWRI activities took place in FY00:

RESEARCH PROJECTS

- Improvement of Water Resources Management Due to Climate Forecasts (sponsored by NOAA); - Climate and Hydrological Forecasts for Operational Water Resources Management, a Demonstration Project (sponsored by NOAA); - Decision Support System for the Alabama-Coosa-Tallapoosa River Basin (sponsored by citizen groups, nature conservancy groups, and US EPA); - Sustainability of Surficial Aquifer Resources on Endmember (Developed and Pristine) Barrier Islands near Brunswick, Georgia (sponsored by USGS); - A Two-Dimensional Hydrodynamic Model for the ACT and ACF River Basins (sponsored by USGS); - Ecological Impacts of Water Management Decisions for the Apalachicola-Chattahoochee-Flint River Basin in a Changing Climate (sponsored by USGS); - Ribotype Source Library of Escherichia Coli Isolates from Georgia (sponsored by USGS); - Water Supply Potential of Seepage Ponds in the Coastal Area of Georgia (sponsored by USGS); - Lake Victoria Decision Support System (LVDSS) Advanced Training Program (sponsored by the World Bank and Governments of Kenya, Tanzania, and Uganda); - A Decision Support Tool for the Nile Basin (sponsored by the Food and Agriculture Organization of the United Nations).

RESEARCH PRODUCTS

GWRI investigators organized and conducted 4 short courses, gave several lectures at local, national and international fora, and supported 16 students through various research projects. In the reporting period, GWRI research resulted in numerous refereed journal publications, conference papers, and water resources research reports. The institute produced two River Basin Decision Support System software packages, one for the South Eastern US, and one for the Lake Victoria region in East Africa. A graduate student internship was continued with the USGS Georgia District, and a graduate student fellowship sponsored by a private company was continued in its second year.

POLICY IMPACT

At the state level, GWRI was involved in many ways in the ongoing tri-state compact negotiation among the states of Alabama, Florida, and Georgia. These three states are negotiating water-sharing agreements for the Alabama-Coosa-Talapoosa (ACT) and Apalachicola-Chattahoochee-Flint (ACF) basins. Under the sponsorship of the US EPA, GWRI performed technical analysis of a draft ACT compact. Assessment results were presented to the Forum of Federal Agencies (including the EPA, US Fish and Wildlife Service, US Army Corps of Engineers, and Southeastern Power Administration) and the ACT-ACF Federal Commissioner. Assessment results have also been requested by U.S. Representative Bob Barr, and numerous federal, state, local, and non-governmental entities.

Significant press coverage has been granted to the GWRI study in newspapers throughout the region, WSB television, and the Associated Press. The final effect of the assessment results on the compact negotiations are not known at this time, but the level of public interest indicates that the impartial technical analysis may have some value for the process. GWRI also sponsored in co-operation with the Upper Chattahoochee Riverkeeper a one-day workshop on technical methods used in the compact process for non-technical stakeholders. Also at the state level, GWRI has proposed a state-wide technology transfer initiative named "Georgia Water-Wise." This program is intended to be a cooperative effort between the academic institutions, various government agencies and bodies at all levels, public interest groups, and private businesses of Georgia who have active interests in the water resources issues of the state. The final form of implementation and funding are currently undecided, but substantial support has been received from all sectors. At the national level, GWRI research projects on the value of climate forecasting in water resources manegent have proven that policy making can indeed benefit from near-term climate prediction. Additionally, the attention generated by GWRI's work in the ACF-ACT compacts process has brought increased appreciation for the role of water resources research and the national Water Resources Research Institutes program. At the international level, GWRI hosted six East African trainees from Kenya, Tanzania, and Uganda at GWRI for extended training in the Lake Victoria Decision Suppport System over a six-month period. GWRI has also been awarded a research contract for a Decision Support Tool for the Nile Basin sponsored by the Food and Agriculture Organization of the United Nations. This project will involve the governments of ten nations and span one of the world's largest river basins.

Research Program

Basic Information

Title:	A Two-Dimensional Hydrodynamic Model for the ACT and ACF River Basins
Project Number:	E-20-F66
Start Date:	3/1/2000
End Date:	2/28/2001
Research Category:	Climate and Hydrologic Processes
Focus Category:	Surface Water, Models, Floods
Descriptors:	Hydrodynamic models, Open-channel flow, Numerical simulation
Lead Institute:	Georgia Institute of Technology
Principal Investigators:	Fotis Sotiropoulos

Publication

A Depth-Averaged Hydrodynamic Model for the ACT and ACF River Basins: Model Development and Validation

by

T. C. Lackey and F. Sotiropoulos

Final Report for Project E-20-F66

Sponsored by

The Georgia Water Resources Institute

Environmental Fluid Mechanics and Water Resources Group
School of Civil and Environmental Engineering
Georgia Institute of Technology
Atlanta GA 30332-0355

Summary

In this report, we develop a two-dimensional hydrodynamic model for simulating swallow-water open-channel flows using depth-averaged equations. The model is capable of handling arbitrarily shaped channel geometries such as those typically encountered in natural rivers. The time-dependent, depth-averaged equations are formulated in generalized, non-orthogonal curvilinear coordinates so that complex river reaches can be accurately modeled using body-fitted computational grids. The equations are discretized in space using a conservative second-order accurate finite-volume method. Adaptive artificial dissipation terms, with scalar and matrix-valued scaling, are explicitly introduced into the discrete equations to ensure that the resulting scheme is applicable to all flow regimes and can accurately capture hydraulic jumps. The discrete equations are integrated in time using a four-stage Runge-Kutta method. For steady-state computations the convergence of the Runge-Kutta algorithm is enhanced using local time stepping, implicit residual smoothing, and multigrid acceleration. Time accurate solutions may also be obtained by integrating the governing equations in time using the four-stage, second-order accurate in time, Runge-Kutta scheme without implementing the aforementioned convergence acceleration measures.

To validate the numerical model, we carry out calculations for a variety of open channel flows for which experimental data have been reported in the literature. The calculated test cases include flow in strongly curved channels and channel expansions. For all cases considered the numerical method is shown to yield solutions of comparable accuracy to those reported in earlier studies in the literature using depth-averaged equations. Discrepancies between predictions and experiments are observed only for very strongly curved channels for which three-dimensional effects dominate.

Due to the lack of detailed bathymetry and flow measurement data for the ACT and ACF basins, the present numerical model was not applied to a real-life reach as was initially intended. This not withstanding, however, the method has been designed to be sufficiently general and its application to a natural geometry is straightforward. The good overall agreement between measurements and numerical simulations for the test cases considered in this report suggests that the present method could serve as a powerful computational tool for understanding the complex flow patterns in the ACT and ACF basins and for guiding the development of simpler one-dimensional models.

Contents

Figures

1. Introduction

The ongoing tri-state (Georgia-Alabama-Florida) negotiations over the allocation of water in the Apalachicola-Chattahoochee-Flint (ACF) and the Alabama-Coosa-Talapousa (ACT) River Basins are presently at a critical stage. Even after, however, a water allocation agreement has been established, there will be a critical need to implement a river management system that ensures that the negotiated water allocation formula is observed by all riparians and that the rivers serve their water users the best way possible. Such an operational management system is not presently in existence. Though the primary emphasis of the tri-state negotiations is placed on droughts, the process also offers an opportunity to apply a modern and more effective flood management system. For the State of Georgia, this is not a luxury but an imperative need in view of the deaths and property damage caused by the killer floods of 1994 and 1996. These severe flooding events underscored the need for developing an operational river management system capable of accurate rainfall estimation, reliable flood forecasting, and effective overall water management. Such a system should be based on remote and on-site data and modern advances in rainfall-runoff, river routing, and reservoir management procedures.

The long-term objective of this research is to develop a two-dimensional numerical model for simulating unsteady flows in the ACF and ACT River Basins. Such a tool is presently necessary in order to: i) study and understand the complex response of the two basins to transient changes in discharge (such as those likely to occur during a hydropower release event and/or a flooding event); and ii) assess the performance and

refine the predictive capabilities of simpler, one-dimensional river routing models used in existing operational river management systems. In this report we develop the hydrodynamic model and demonstrate its predictive capabilities by applying it to calculate several benchmark open-channel flow cases for which experimental data are available in the literature.

This report is organized as follows. First, we review the literature and discuss previous work on depth-averaged numerical modeling. Subsequently, we present the governing equations in Cartesian and curvilinear coordinates and then describe in detail the numerical method we developed for solving those equations. This is followed by the presentation of numerical results for a number of test cases we employed to validate the method. Finally we summarize our findings and discuss future data needs for applying the numerical model to the ACT and ACF basins.

2. Review of Previous Work

Depth-averaged models have been employed in the past to simulate flows in man-made open channels as well as in natural environments, such as river systems and estuaries. We present here a brief review of previous numerical studies including works that focused on shallow flows both in man-made and natural environments. It should be pointed out that what follows is not intended to be an extensive review of related literature. We rather focus on few studies that underscore the progress made in modeling open channel flows with 2D models during the past decade.

Among the most notable early studies is the work of Tingsanchali and Rodi (1986) who developed a depth-averaged k-ε model for simulating suspended sediment transport in the Neckar River in Germany. Wenka et al. (1991) employed a similar k-ε model to simulate flooding over a stretch of the river Rine in Germany. They reported good agreement between the predicted flow patterns and those observed in aerial photographs of the river during the flooding event. Younus and Chaudhry (1994) developed a depth-averaged k-ε turbulence model and applied it to various channel geometries including circular hydraulic jumps. They reported significant improvements in the agreement between experiments and computations for the hydraulic jump simulations using the k-ε model. Muin and Spaulding (1996) developed a two-dimensional model for simulating tidal circulation patterns in the Providence River. Their model neglects all viscous and turbulent stresses, except, of course, the stresses due to bed friction. Hu and Kot (1997) developed a depth-averaged model for studying tides in the Pearl River estuary in China. They employed the constant eddy-viscosity

assumption for turbulence closure. Shankar and Cheong (1997) employed various formulations of a 2D numerical model to study tidal motions in Singapore coastal waters. They also adopted the constant eddy-viscosity assumption. Molls and Zhao (2000) considered supercritical flow in channels with a wavy sidewall using the 2D depth-averaged equations and neglecting the depth-averaged viscous stresses. They investigated the effect of bottom friction, effective stresses, artificial viscosity, and channel geometry. Panagiotopoulos and Soulis (2000) developed an implicit bidiagonal scheme for the depth-averaged free-surface flow equations, in an effort to further increase the efficiency of 2D numerical models. They also neglected viscous stresses.

In this work, we develop a 2D, depth-averaged model capable of simulating flows in natural geometries. The model is formulated in generalized curvilinear coordinates to allow accurate description of arbitrarily complex geometries using body-fitted grids. The governing equations are discretized in strong-conservation form using a second-order accurate finite-volume method with explicitly added adaptive artificial dissipation terms. An explicit Runge-Kutta algorithm is used to integrate the governing equations in time. Convergence to steady state is enhanced using local time-stepping, implicit residual smoothing, and multigrid acceleration. The predictive capabilities of the model are demonstrated by applying it to calculate several benchmark test cases for which experimental data is available in the literature.

3. The Numerical Method

In the following sections, we present the depth-averaged open-channel flow equations and describe the numerical method we employ to solve the governing equations.

3.1 Governing Equations

The numerical model solves the unsteady, depth-averaged, open-channel flow equations. These equations are obtained by integrating the three-dimensional, incompressible, Navier-Stokes from the river bed to the water surface under the following assumptions: i) uniform velocity distribution in the depth direction; ii) hydrostatic pressure distribution; iii) small-channel bottom slope; iv) negligible wind shear at the surface; v) negligible viscous stresses except stresses due to bed friction; and vi) negligible Coriolis acceleration. Although this averaging procedure simplifies the equations considerably, information concerning the vertical variations of the velocity distribution is lost. Nevertheless, the depth-averaged equations have been shown to yield very good predictions for flows in shallow channels and provide a far more practical, from the computational standpoint, engineering alternative to the full, three-dimensional Navier-Stokes equations.

The depth-averaged open-channel flow equations (continuity and momentum) formulated in Cartesian coordinates read in flux-vector format as follows (see Kuipers and Vreugdenhil (1973) for the details of the integration):

$$\frac{\partial \hat{Q}}{\partial t}+\frac{\partial \hat{F}}{\partial x}+\frac{\partial \hat{G}}{\partial y}=\hat{H} \tag{1}$$

where the flux vectors are defined as follows:

$$\hat{Q}=\begin{bmatrix} h \\ hu \\ hv \end{bmatrix} \; ; \quad \hat{F}=\begin{bmatrix} hu \\ hu^2+\frac{gh^2}{2} \\ huv \end{bmatrix}; \hat{G}=\begin{bmatrix} hv \\ huv \\ hv^2+\frac{gh^2}{2} \end{bmatrix}; \quad \hat{H}=\begin{bmatrix} 0 \\ gh(S_{ox}-S_{fx}) \\ gh(S_{oy}-S_{fy)} \end{bmatrix} \tag{2}$$

In the above systems the first row is the continuity equations, while the second and third rows are the x-momentum and y-momentum equations, respectively. The variable *h* is the water depth, *u* and *v* are the depth-averaged velocity components in the *x*- and *y*-directions, respectively, and *g* is the acceleration of gravity. The bottom slopes S_{ox} and S_{oy} are defined as

$$S_{ox}=-\frac{\partial z}{\partial x} \; ; \qquad S_{oy}=-\frac{\partial z}{\partial y} \tag{3}$$

where *z* is the channel bottom elevation. The friction slopes S_{fx} and S_{fy} in the x- and y-direction are defined as

$$S_{fx}=\frac{n^2 u\sqrt{(u^2+v^2)}}{h^{4/3}}; \qquad Sy=\frac{n^2 v\sqrt{(u^2+v^2)}}{h^{4/3}} \tag{4}$$

where *n* is the Manning's flow friction coefficient.

To facilitate the description of natural geometries using body-fitted grids, the above equations are transformed from Cartesian to generalized curvilinear coordinates by invoking the partial transformation approach $(x, y) \rightarrow (\xi, \eta)$, which maintains the Cartesian velocity components as the dependent variables. The transformed equations read as follows:

$$\frac{\partial Q}{\partial t} + \frac{\partial F}{\partial \xi} + \frac{\partial G}{\partial \eta} = H \tag{5}$$

where

$$Q = \frac{\hat{Q}}{J} \quad F = \frac{(\hat{F}\xi_x + \hat{G}\xi_y)}{J} \quad G = \frac{(\hat{F}\eta_x + \hat{G}\eta_y)}{J} \quad H = \frac{\hat{H}}{J} \tag{6}$$

in which J is the Jacobian of the geometric transformation given by

$$J = \frac{1}{x_\xi y_\eta - x_\eta y_\xi} = \xi_x \eta_y - \xi_y \xi_x \tag{7}$$

where the transformation metrics are related with each other via the following relations:

$$\frac{\partial \xi}{\partial x} = J \frac{\partial y}{\partial \eta} \qquad \frac{\partial \xi}{\partial y} = -J \frac{\partial x}{\partial \eta}$$

$$\frac{\partial \eta}{\partial x} = -J \frac{\partial y}{\partial \xi} \qquad \frac{\partial \eta}{\partial x} = J \frac{\partial x}{\partial \xi} \tag{8}$$

The velocity components *u* and *v* in the physical domain are related to the U and V contravariant velocity components with the following equations:

$$U = \frac{\partial \xi}{\partial x} u + \frac{\partial \xi}{\partial y} v ; \quad V = \frac{\partial \eta}{\partial x} u + \frac{\partial \eta}{\partial y} v \tag{9}$$

The Jacobian matrices of the flux vectors *E* and *F*, whose eigenvalues will be used in the formulation of the artificial dissipation model described in the subsequent section, are defined as follows:

$$A = \frac{\partial E}{\partial Q} = \begin{bmatrix} 0 & \xi_x & \xi_y \\ c^2 \xi_x - uU & U + u\xi_x & u\xi_y \\ c^2 \xi_y - vU & v\xi_x & U + v\xi_y \end{bmatrix}$$

$$B = \frac{\partial F}{\partial Q} = \begin{bmatrix} 0 & \eta_x & \eta_y \\ c^2 \eta_x - uV & V + u\eta_x & u\eta_y \\ c^2 \eta_y - vV & v\eta_x & V + v\eta_y \end{bmatrix} \tag{10}$$

The eigenvalues of A and B are given as follows:

$$\lambda_1^A = U \qquad \lambda_2^A = U + c\sqrt{\xi_x^2 + \xi_y^2} \qquad \lambda_3^A = U - c\sqrt{\xi_x^2 + \xi_y^2} \tag{11}$$

$$\lambda_1^B = V \qquad \lambda_2^B = V + c\sqrt{\eta_x^2 + \eta_y^2} \qquad \lambda_3^B = V - c\sqrt{\eta_x^2 + \eta_y^2}$$

where *c* is the wave celerity $c = \sqrt{gh}$.

3.2 Spatial discretization scheme

The depth-averaged continuity and momentum equations are formulated in strong-conservation form and discretized using the finite-volume approach. Using second-order accurate central differencing to discretize all spatial derivatives, a semi-discrete form of equation (5) can be written as follows:

$$\frac{dQ_{ij}}{dt} + R_{ij} = 0 \tag{12}$$

where

$$R_{ij} = \frac{\tilde{E}_{i+1/2,j} - \tilde{E}_{i-1/2,j}}{\Delta\xi} + \frac{\tilde{F}_{i,j+1/2} - \tilde{F}_{i,j-1/2}}{\Delta\eta} - H_{ij} \tag{13}$$

The convective flux vectors at the cell interfaces are approximated in the following general manner:

$$\tilde{E}_{i+1/2,j} = \frac{1}{2}\left(E_{i,j} + E_{i+1,j}\right) + D^{\xi}_{i+1/2,j} \tag{14}$$

where $D^{\xi}_{i+1/2,j}$ is an artificial dissipation flux necessary for eliminating odd-even (grid scale) oscillations associated with the dispersive three-point central differencing scheme (obtained by setting $D^{\xi}_{i+1/2,j}$=0 in eqn. (14)) and for capturing hydraulic jumps.

We implement herein a non-linear artificial dissipation model by extending to depth-averaged flows techniques developed for capturing shock waves in compressible flows (see Jameson et al. 1981). More specifically, the artificial dissipation flux consists

of a blend of both first and third-order terms, each multiplied by appropriate functions designed to switch-on or off certain terms based on the local intensity of the spatial gradients of the water elevation. Thus, in regions of steep water-surface gradients (i.e. near hydraulic jumps) the first-order terms are automatically turned on by the model to preserve the robustness and monotonicity of the numerical model. In smooth regions of the flow, however, only the third-order terms are activated, thus, preserving the second-order accuracy of the numerical method. The dissipative term for the *i* direction is given as follows:

$$D^{\xi}{}_{i+\frac{1}{2},j} = \rho(A)_{i+\frac{1}{2},j}\left[\varepsilon^{(2)}_{i+\frac{1}{2},j}\left(Q_{i+1,j} - Q_i\right) - \varepsilon^{(4)}_{i+\frac{1}{2},j}\left(Q_{i+2,j} - 3Q_{i+1,j} + 3Q_{i,j} - Q_{i-1,j}\right)\right] \qquad (15)$$

where ρ(A) is the spectral radius of the Jacobian matrix A

$$\rho(A) = |U| + c\sqrt{\xi_x^2 + \xi_y^2} \qquad (16)$$

and $\varepsilon^{(2)}$ and $\varepsilon^{(4)}$ are non-linear functions of the water-surface gradient parameter ν_i as follows:

$$\nu_i = \frac{\left|h_{i+1,j} - 2h_{i,j} + h_{i-1,j}\right|}{h_{i+1,j} + 2h_{i,j} + h_{i-1,j}} \qquad (17)$$

$$\varepsilon^{(2)}_{i+\frac{1}{2},j} = \kappa^{(2)} \max\left(\nu_{i+1}, \nu_i\right) \qquad (18)$$

$$\varepsilon^{(4)}_{i+\frac{1}{2},j} = \max\left\{0, \left[\kappa^{(4)} - \varepsilon^{(2)}_{i+\frac{1}{2},j}\right]\right\} \qquad (19)$$

where $\kappa^{(2)}$ and $\kappa^{(4)}$ are constants with values of .5 and .1 respectively. The terms in the *j*-direction are constructed in a similar manner.

3.3 Temporal integration scheme

The discrete governing equations (12) are integrated in time using the following explicit, four-stage, Runge-Kutta algorithm (for k=1,2,3,4):

$$Q_{ij}^{k} = Q_{ij}^{n} - \alpha_k \Delta t R_{ij}^{k-1} \tag{20}$$

where $Q^{(1)} = Q^{n}$ and $Q^{(4)} = Q^{n+1}$, n denotes the current time level, α_k are the Runge-Kutta coefficients (=1/4, 1/3, 1/2, and 1 for k=1,2,3,4), and Δt is the time increment. The above algorithm is second-order accurate in time and can be used to integrate the governing equations in a time-accurate manner. In spite of the fact that it is explicit, and thus imposes time-step limitations as compared to fully implicit procedures, the Runge-Kutta scheme is selected herein because it can take full advantage of parallel computer architectures. The present algorithm does not involve matrix inversion operations and can, thus, be parallelized very effectively and in a rather straightforward manner. The resulting computer code is able to run very efficiently on multi-processor computer architectures and, thus, the additional cost due to the increased number of time steps required to simulate a given time interval (because of the stability restriction of the explicit algorithm) is greatly offset by the drastic reduction of CPU time per time step.

For steady-state computations, the convergence rate and thus the efficiency of the explicit algorithm given by eqn. (20) can be greatly enhanced by implementing local time-stepping, implicit residual smoothing and multigrid acceleration. These convergence enhancement measures are described in the subsequent sections.

3.3.1 Local Time Stepping

If only steady-state solutions are of interest, local time-stepping can be employed to ensure that the damping properties of the iterative algorithm are optimized by maintaining a constant Courant-Friedrich-Lewis (CFL) number at every grid node. The local time steps are calculated as follows:

$$\Delta t_{ij} = \frac{CFL}{\max\left[\rho(A)_{i,j}, \rho(B)_{i,j}\right]} \tag{21}$$

At every grid node, the local time increment is updated once every time step and is employed in place of Δt in eqn. (20).

3.3.2 Implicit Residual Smoothing

The stability and robustness of the iterative algorithm given by eqn. (20) can be greatly enhanced by implementing the implicit residual smoothing procedure proposed by Jameson et al. (1981). The Runge-Kutta scheme with local time stepping and implicit residual smoothing reads as follows:

$$\Im\left(\Delta Q_{ij}^{k}\right) = -\alpha_k \Delta t_{ij} R_{ij}^{k-1} \tag{22}$$

$$Q^{k} = Q^{n} + \Delta Q^{k} \tag{23}$$

where $\Im$ is the implicit residual smoothing operator defined as follows:

$$\Im(\ ) = \left(1-\varepsilon_1 \delta_{\xi\xi}\right)\left(1-\varepsilon_2 \delta_{\eta\eta}\right) \tag{24}$$

and ε_1 and ε_2 are positive constants of order one and $\delta_{\xi\xi}$ is the three-point, central, finite difference operator for the second order derivative.

3.3.3 Multigrid Acceleration

A typical multigrid method applies an iterative scheme (the so-called smoother) with good damping properties of the high frequency components of the error to successively coarser grids. Since coarser grids allow the use of larger time-steps, the resulting algorithm can efficiently damp the entire spectrum of error frequencies, thus, yielding rapid convergence rates. Perhaps the most attractive feature of the multigrid method is that, when properly formulated, its convergence rate does not depend on the size of the system to be solved. In the present study, the non-linear Full Approximation Storage Scheme (FAS) proposed by Brandt (1977) is employed in conjunction with the multigrid strategy proposed by Jameson (1983, 1985) for the solution of the Euler equations and applied to the depth-averaged equations. The overall method is described below.

Two coarsening strategies are commonly used to construct the series of successively coarser grid required for the multigrid method. In the full-coarsening strategy, coarser grids are constructed by eliminating every other node in all coordinate directions; whereas, in the semi-coarsening strategy only nodes in some of the coordinate directions are eliminated. Starting with an estimate of the solution on the finest grid, the flow variables are transferred (or restricted) to the coarser grid using injection, that is, a transfer operator $T^{s}_{h,2h}$ which picks flow variables at alternate points to define coarse grid flow data as well as the coarse grid coordinates:

$$Q^{(n)}_{2h} = T^{s}_{2h,h} Q_h \tag{25}$$

where, the subscripts *h* and *2h* denote fine and coarse grids, respectively. To prevent errors introduced by solving the equations on the coarse grid from ultimately contaminating the fine-grid solution, a forcing term $\wp_{2h}$ is added to the coarse grid equations:

$$\wp_{2h} = T^{r}_{2h,h} R_h(Q_h) - R_{2h}(Q^{(n)}_{2h}) \tag{26}$$

where $T^{r}_{2h,h}$ is the residual restriction operator. This operator is computed using a weighted average of all the *h*-grid nodes that surround a particular *2h*-grid node as follows:

$$T^{r}_{2h,h} = \mu^{2}_{\xi} \mu^{2}_{\eta} \tag{27}$$

where the operator μ^2_ξ averages the residual in the ξ-direction. In two dimensions, the above operator is written as follows:

$$\mu_\xi^2 \mu_\eta^2 \left[R_h(Q_h)\right]_{i,j} = \tfrac{1}{4}\mu_{\xi^1}^2 \left[R_h Q_h\right]_{i,j-1} + \tfrac{1}{2}\mu_\xi^2 \left[R_h Q_h\right]_{i,j} + \tfrac{1}{4}\mu_\xi^2 \left[R_h Q_h\right]_{i,j+1} \tag{28}$$

which when expanded yields

$$\begin{aligned} \mu_\xi^2 \mu_\eta^2 \left[R_h(Q_h)\right]_{i,j} = {} & \tfrac{1}{16} R_h(Q_h)_{i-1,j-1} + \tfrac{1}{8} R_h(Q_h)_{i,j-1} + \\ & \tfrac{1}{16} R_h(Q_h)_{i+1,j-1} + \tfrac{1}{8} R_h(Q_h)_{i-1,j} + \\ & \tfrac{1}{4} R_h(Q_h)_{i,j} + \tfrac{1}{8} R_h(Q_h)_{i+1,j} + \\ & \tfrac{1}{16} R_h(Q_h)_{i+1,j-1} + \tfrac{1}{8} R_h(Q_h)_{i-1,j} + \\ & \tfrac{1}{16} R_h(Q_h)_{i+1,j+1} \end{aligned} \tag{29}$$

With the forcing added to the Runge-Kuttta procedure, the algorithm used for the coarse-grid equations becomes

$$Q_{2h}^k = Q_{2h}^{(n)} - \alpha_k \Delta t_{ij} \Im^{-1}(R_{2h}^{k-1} + \wp_{2h}) \tag{30}$$

A V-cycle cycling strategy is used to characterize the order in which the data is transferred from grid to grid. In the V-cycle, the equations are solved using the Runge-Kutta method on the *h* grid, and the data is injected to the *2h* grid. The equations are then

solved on *2h* grid and injected to the *4h* grid, and so on until the coarsest grid level is reached. Once the coarsest grid is reached, the solution on the coarsest grid must be prolonged back to the *h* (fine) grid via the *2h* grid before another time step can begin. If Q_{2h}^{+} is the solution vector on the *2h* grid that was prolonged from the *4h* grid, then the solution vector on the *h* grid is

$$Q_h^{+} = Q_h + I_{h,2h}(Q_{2h}^{+} - Q_{2h}^{(0)}) \tag{31}$$

where $I_{\mathrm{h,2h}}$ is an interpolation operator. The correction on the *2h* grid is transferred to the *h* grid via injection for common nodes. A simple averaging procedure is used for the interpolation operator. To eliminate high-frequency errors that may be introduced by this interpolation procedure, the interpolated solutions are smoothed using implicit residual smoothing before being prolonged back to the fine grid. A smoothing operator can be incorporated into the equation for Q_h^{+} by writing

$$Q_{2h}^{+} = Q_h + \Delta Q_{h,2h}^{+} \tag{32}$$

where

$$\Delta Q_{h,2h}^{+} = \Im^{-1}[I_{h,2h}(Q_{2h}^{+} - Q_{2h}^{(0)})] \tag{33}$$

and $\Im$ is the smoothing operator, which is used exclusively during prolongation.

A three-level V-cycle with subiterations is used in the present study for each time step on the finest mesh. One iteration is performed on the h grid, two on the 2h grid, and

three on the 4h grid. On all coarse meshes a constant-coefficient, first-order accurate, second-difference artificial dissipation term is employed. This simplification does not affect the accuracy of the fine grid solution—the forcing term introduced in the coarse mesh equations ensures that coarse-mesh corrections are driven by fine mesh residuals—but it enhances the robustness of the overall algorithm.

3.4 Boundary conditions

Boundary conditions are separated into two cases: supercritical and subcritical flow conditions. For supercritical cases, at the inlet, the *u* (longitudinal) velocity, the *v* (transverse) velocity , and the water depth *h* are all specified and do not change during computations. At the outlet, all variables are extrapolated from the interior points. For subcritical cases, at the inlet, the *u* and *v* velocities are specified and *h* is extrapolated from the interior point. At the outlet the depth, *h*, is specified and the velocities *u* and *v* are extrapolated from the interior points.

For both cases the channel side walls are treated in the same manner. Free-slip boundary conditions are implemented by setting the contravariant velocity component U_{wall} equal to U at the first interior point. The condition of no mass flow perpendicular to the solid wall is then applied by setting the contravariant velocity component V_{wall} to be zero. The water depth, h, is extrapolated from the interior points.

4. Validation and Application of the Numerical Model

To validate the numerical model and demonstrate its predictive capabilities, we applied it to simulate four cases for which experimental data have been reported in the literature. These cases span all possible flow regimes, from supercritical to subcritical flow, and simulate various types of channel geometries. The details for each case along with comparisons of the computed results with both experimental studies and previous numerical computations are described in the following section.

4.1 Case 1: Channel Expansion at F=2.0 (Rouse et al. 1951)

The computational grid for this case is shown in figure 1. The curved wall of this channel is described by the following equation:

$$\frac{y}{b_1} = \frac{1}{2}\left(\frac{x}{2b_1}\right)^{3/2} + \frac{1}{2} \tag{34}$$

where b_1 is the channel width and has a value of 10.0m at the entrance. The channel is symmetrical about the horizontal centerline, so only the upper half portion is modeled and symmetry boundary conditions are applied at y=0. The computational grid is 61 x 21. The inlet water depth h_1 is 1.0m and the Froude number ($F=u/(gh)^{0.5}$) is 2.0. The value of the Manning's flow friction coefficient was 0.012 and the values of S_{ox} and S_{oy} of 0.0.

Figure 2 shows the comparison of the experimental water depth along the channel axial distance (Rouse 1957) and the corresponding numerical model results. The comparisons are satisfactory for both the curved line and the midstream line. The Froude

number is supercritical throughout the flow field and, thus, the flow is accelerating as expected. Some discrepancies between experiments and computations are only observed along the curved wall of the channel near the exit, where the predicted water depth is somewhat higher than measured. As discussed in Panagiotopoulos et al. (2000), however, this discrepancy should be attributed to the growth of the boundary layer along the curved wall, a process that can not be modeled with the present inviscid model.

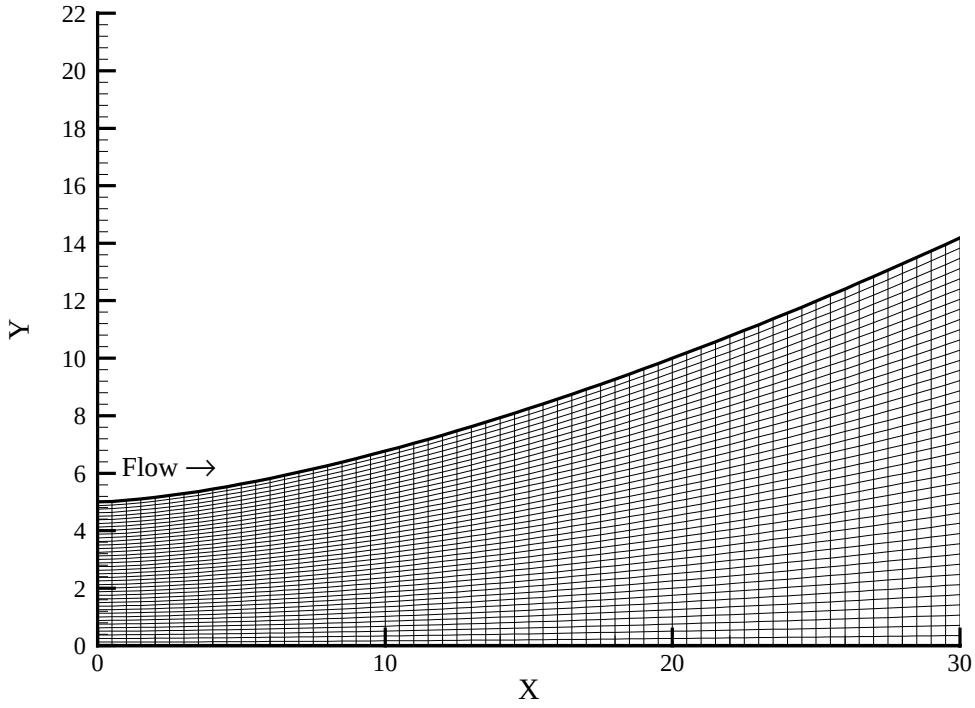

Figure 1. Grid and channel geometry for Case 1.

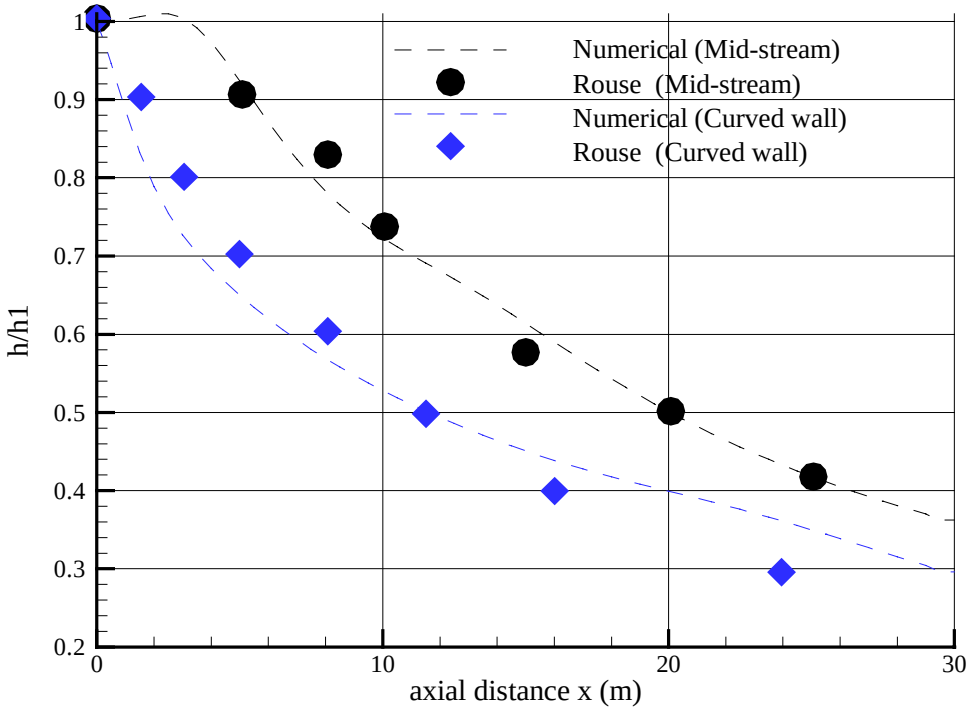

Figure 2. Measured (Rouse et. al 1951) and predicted water surface profiles along the inner and outer banks for Case 1.

4.2 Case 2: 180-deg bend, R_c/B=1.5, F=0.338 (Rozovskii 1957)

This case represents the first of the two Rozovskii experiments discussed in this report. The computational domain consists of a 6.0m long straight approach channel, a 180-degree bend with R_c/B=1.5 (where R_c is the mean radius of curvature and B is the channel width), and a 3.0m long exit channel. The Manning's n value used in this simulation is 0.00925. The width to inlet depth radio is 0.075. The inlet depth is h_{inlet} = 60mm and B is 0.8m. The velocity at the inlet is uniform and equal to 0.26m/s and the Froude number is 0.338. The computations were performed on a grid, as seen in figure 3, with 124 x 21 nodes in the longitudinal and transverse directions, respectively.

Figure 4, shows the comparison between the calculated and measured longitudinal water surface profiles along the inner and outer walls of the bend. As seen the numerical simulations capture the general trends observed in the measurements with reasonable accuracy, especially along the outer bank. Some discrepancies are observed, however, along the inner bank where the model underestimates the measured water depth. It is important to note that the present 2D results are actually very similar to those obtained by Meselhe and Sotiropoulos (2000) for the same geometry using a fully 3D turbulent flow numerical model with deformable free-surface. They too reported an underestimation of the water depth along the inner bank and attributed this deficiency to the inability of their turbulence model to resolve correctly the strength of the secondary motion, which is responsible for redistributing momentum within the channel cross-section.

Figure 5 compares measured and calculated streamwise velocity profiles at several streamwise sections upstream, within, and downstream of the bend. With only exception the θ=0 section, where the model overestimates the velocity near the outer bank, the

computed profiles are in very good overall agreement with the measurements. The discrepancies at the θ=0 section could be due to viscous effects due to the thickening of the boundary layer along the straight upstream segment. Interestingly, the present results are at least as good as the 3D, turbulent flow computations by Meselhe and Sotiropoulos (2000). The fact that for such a complex flow the present model can yield results of accuracy comparable to a full 3D model is very encouraging and suggest that the model can be a powerful and very efficient tool for studying flow patterns in natural rivers.

The effect of the multigrid method in the convergence rate of the numerical algorithm is demonstrated in Figure 6, which compares the convergence histories for the single grid algorithm, multigrid with semi-coarsening, and multigrid with full coarsening. As seen in this figure multigrid in conjunction with an optimal grid coarsening strategy can accelerate the convergence to steady state by more than 50 percent.

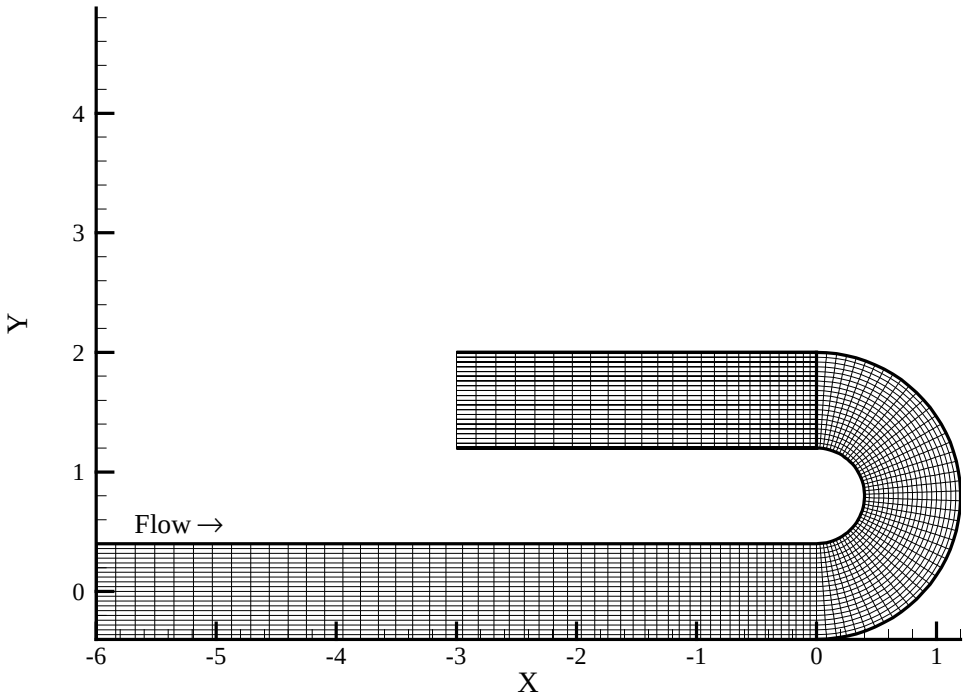

Figure 3. Grid and channel geometry for 180 degree bend with 0.8 radius of curvature.

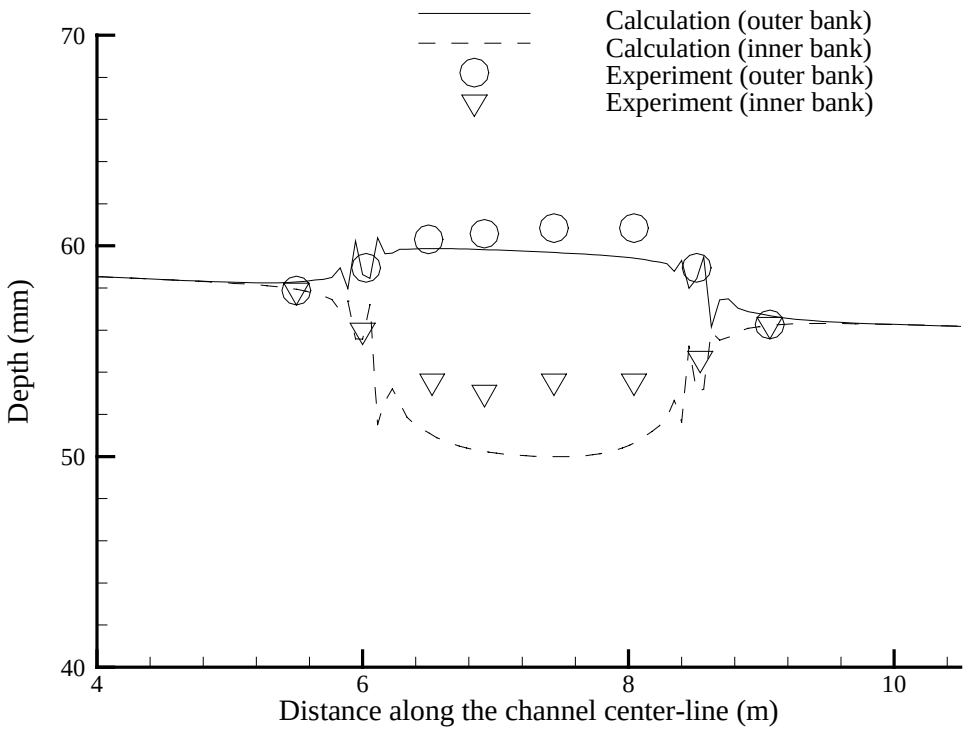

Figure 4. Measured and predicted (Rozovskii 1965) water surface profiles along the inner and outer banks for Case 2.

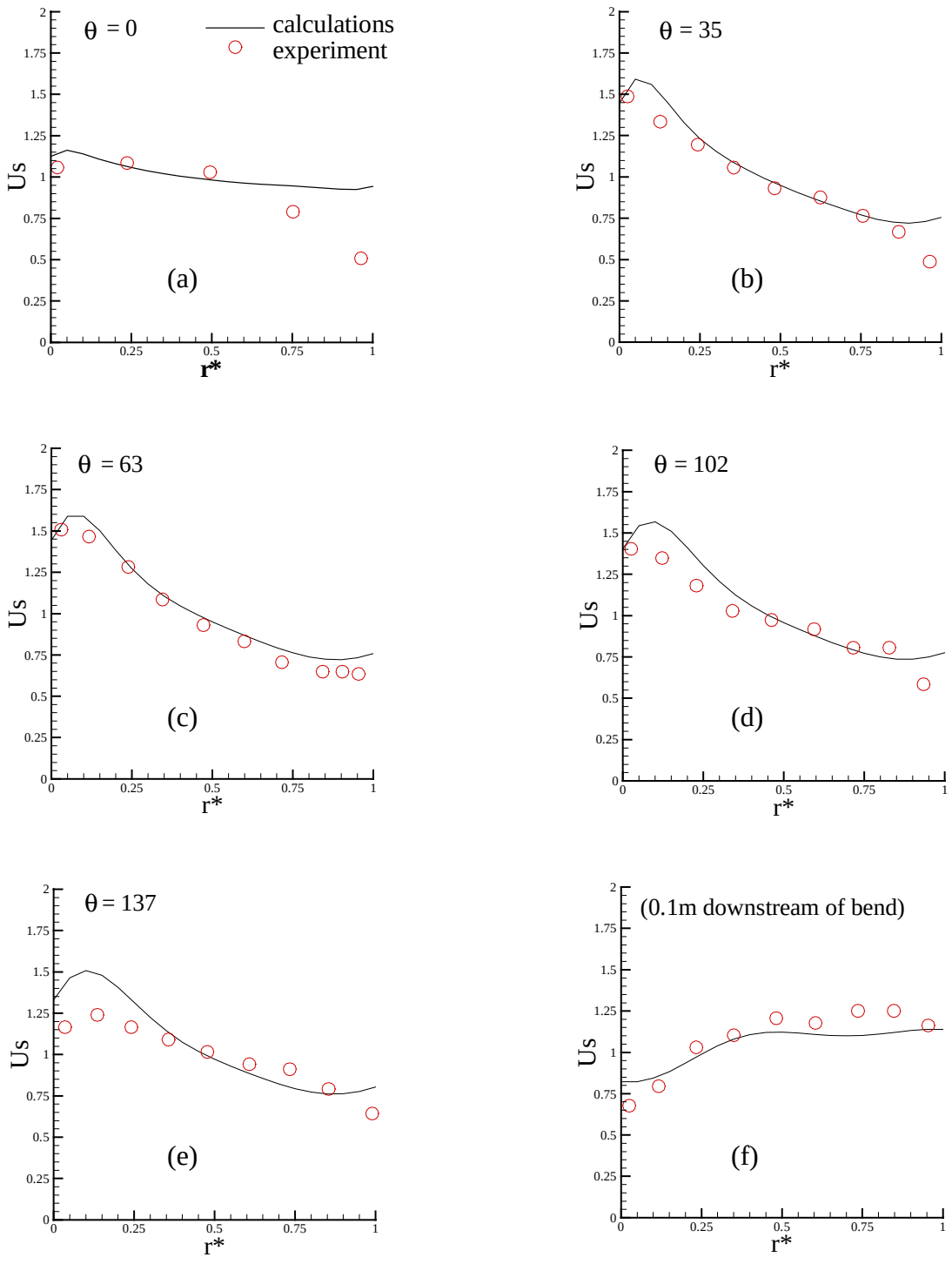

Figure 5. Measured and predicted depth-averaged streamwise velocity profiles at selected cross-sections for Case 2, where $r^*=(r-r_{inner})/B$.

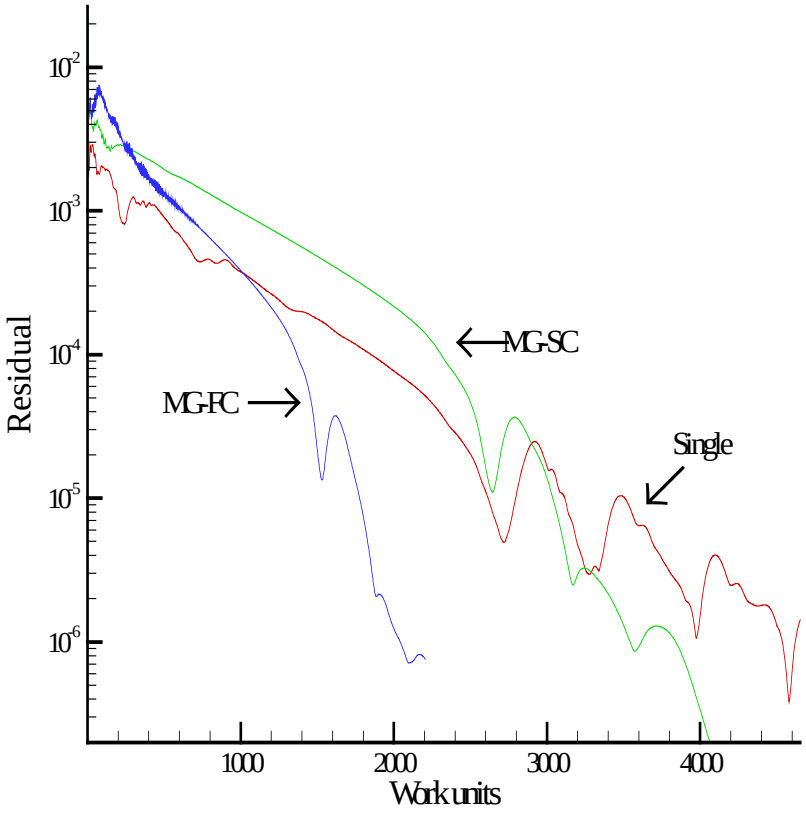

Figure 6 Convergence histories for multigrid vs. single grid computations for Case 2. MG-FC is the multigrid method with full coarsening and MG-SC is the multigrid method with semi-coarsening. Single represents the single grid method.

4.3 Case 3: 180-deg bend, R_c/B=1.0, F=0.114 (Rozovskii 1965)

The second channel geometry studied experimentally by Rozovskii is also a 180 degree bend but with considerably larger radius of curvature—R_c/B = 1.0. The depth-to-width ratio at the inlet is h/B = 0.075 and the Froude number at the inlet is 0.114. The value of the friction coefficient is 0.005 and the calculations were performed on a 160 x 21 computational grid shown in figure 7. Rozovskii reported experimental measurements for water surface profiles, surface elevation contours, and depth-averaged mean velocity profiles.

In figure 8, we plot the variation of the water surface superelevation as a percentage of the inlet depth, η, along the inner and outer banks of the channel. The figure includes the experimental results of Rozovskii, the present 2D simulations, and the results of a fully 3D, turbulent flow calculation by Leschziner and Rodi (1979). Our results are in reasonable agreement with the measurements along the outer bank. Along the inner bank, on the other hand, our computations underpredict somewhat the measured water depth, in a manner similar to that observed in the previous case (see figure 4). Interestingly the 2D results are actually comparable to the 3D simulations of Leschziner and Rodi (1979), with the 3D model performing better along the inner bank of the channel. The inability of the 2D model to predict correctly the water depth near the inner bank should be attributed to the strong secondary motion that develops within the bend due to the transverse gradients of the water-surface elevation. The secondary motion is direct from the outer to the inner bank along the bed and acts to transport low momentum fluid toward the inner bank.

Measured and computed depth-averaged streamwise velocity profiles are compared with each other in figure 9. The calculations capture the general measured trends with reasonable accuracy but the agreement with the measurements deteriorates considerably near the inner bank as the exit of the bend is approached. The observed overprediction of the velocity near the inner bank is in fact consistent with the underprediction of the water depth in order for mass to be conserved. Once again these discrepancies should be attributed to the three-dimensional effects of the secondary motion, which can not be accounted for with a 2D model. Interestingly the numerical model appears to perform better for the previous test case (compare figures 5 and 9) for which the bend curvature is milder and, thus, the secondary motion should be weaker than that generated within the present strongly curved bend.

Figure 10 shows a comparison of the surface elevation contours for the experimental Rozovskii data, the three dimensional numerical Leschziner prediction, and the two dimensional numerical model.

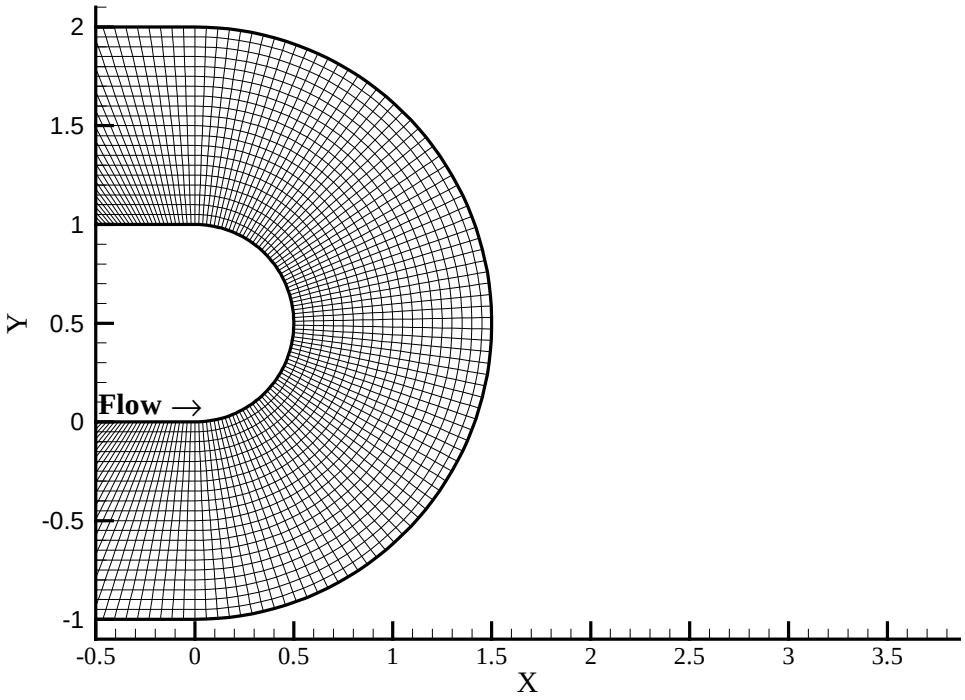

Figure 7. Grid and channel geometry for Case 3.

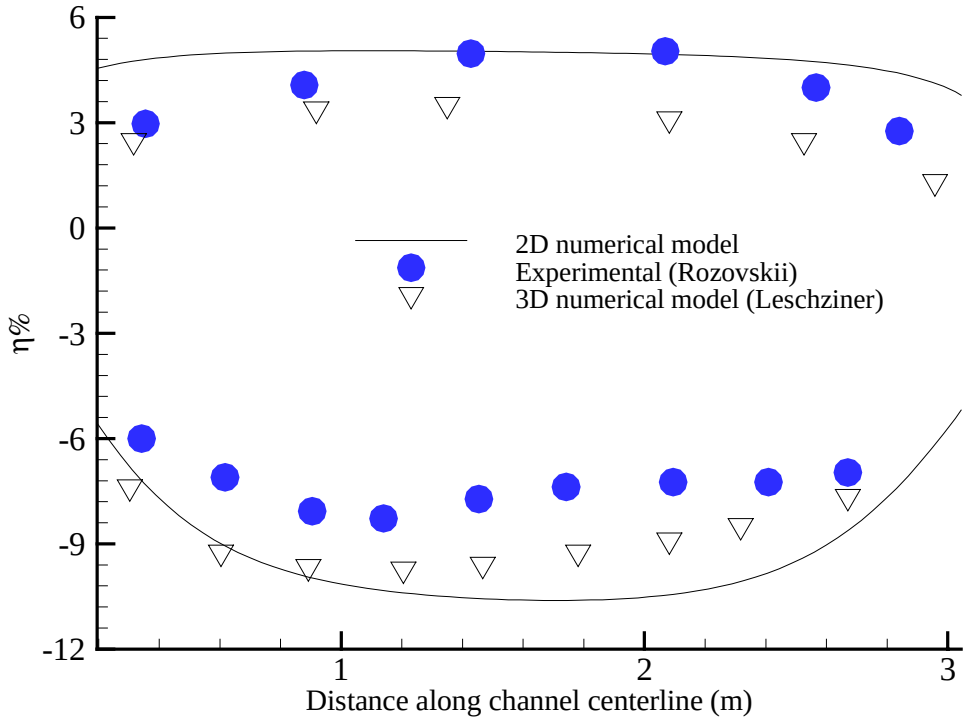

Figure 8. Measured and predicted water surface profiles along the inner and outer banks for Case 3. The symbol, η represents the water surface superelevation relative to the inlet depth.

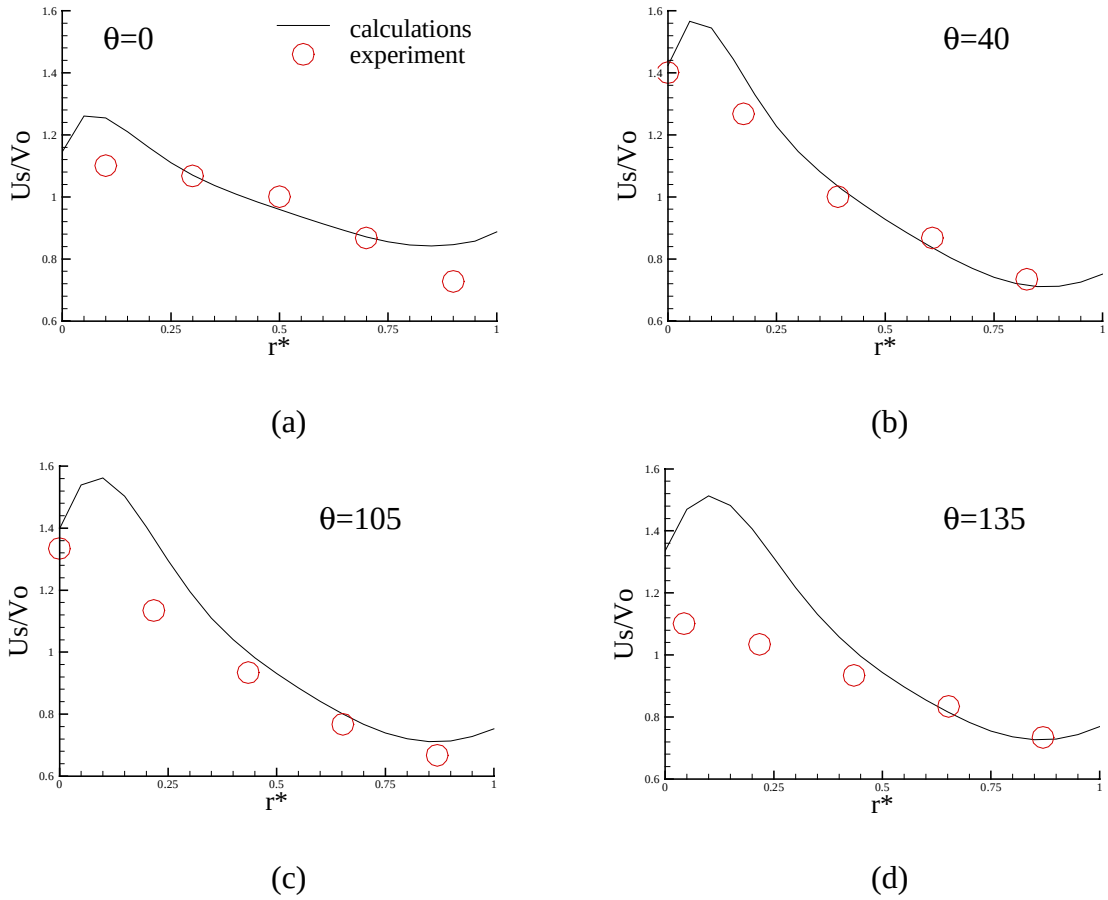

Figure 9. Measured and predicted depth-averaged streamwise velocity profiles at selected cross-sections for Case 3, where $r^*=(r-r_{inner})/B$.

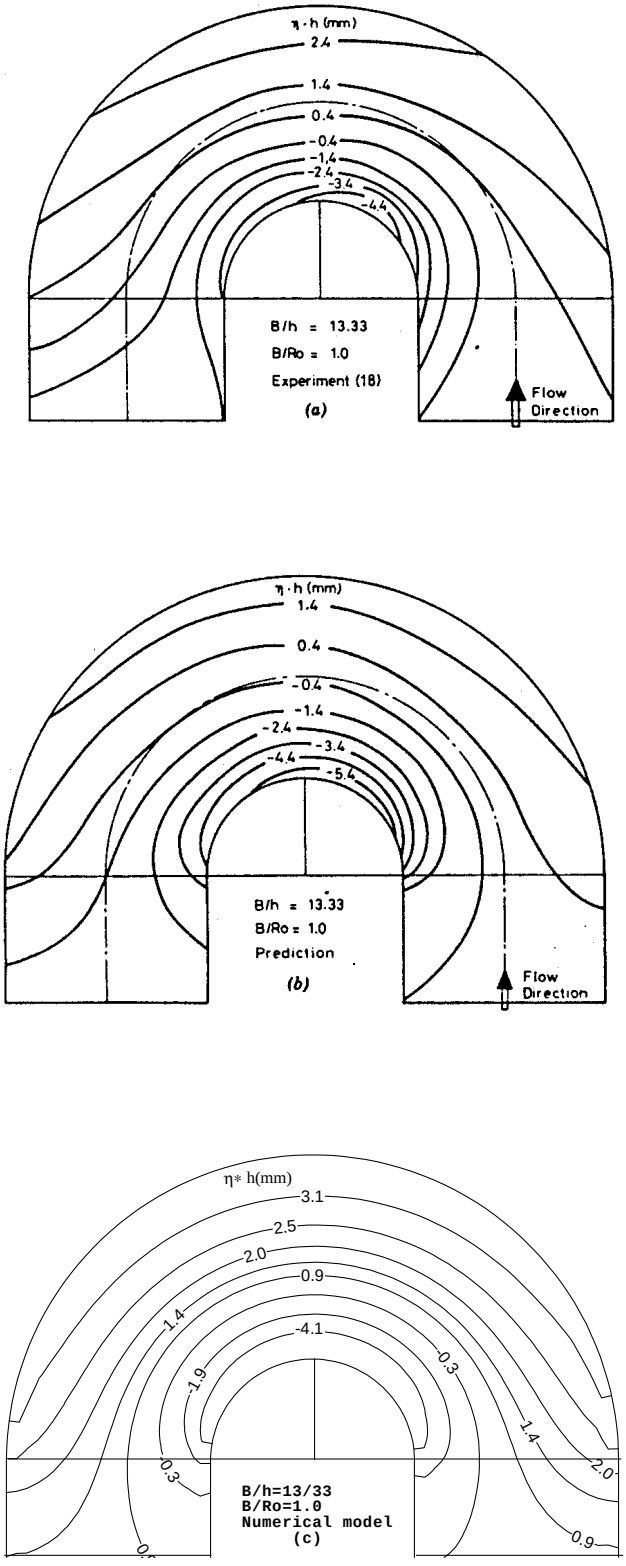

Figure 10. Measured and predicted superelevation contours for Case 3: a) Rozovskii experimental results, b) 3D numerical model (Leschziner 1979), c) 2D numerical model.

4.4 Case 4: Hydraulic jump in a diverging rectangular channel

With this test case we demonstrate the ability of the numerical model to capture hydraulic jumps in open channel flows. The experiment was carried out by Khalifa (1980) for the diverging channel configuration shown in figure 11. The supercritical flow inlet conditions *h*, *u*, *v* were specified as 0.0976m, 1.94m/s, and 0m/s, respectively. At the downstream end the flow is subcritical. Boundary conditions for the velocity components *u* and *v* were specified at the exit as 0.302m/s and 0.0m/s, respectively, while the water surface elevation *h* was extrapolated from the interior points. The computational grid can be seen in Figure 7a and consists of 61 x 21 grid nodes.

The calculated steady-state water-surface profile along the channel centerline is compared with the experimental measurements of Khalifa (1980) in figure 12. The numerical model captures correctly both the location of the jump and the overall change in water depth across the jump. The main discrepancy between the computations and the measurements is that the latter indicate a more gradual transition—i.e. the measured thickness of the jump is somewhat larger than computed. This could be due to viscous effects that would tend to spread the jump and are not accounted for in the present numerical model. We may also speculate that difficulties in obtaining accurate experimental data across the jump (due to very strong turbulence at the water surface) may also be partly responsible for the observed discrepancies. Note that the same case was also computed by Younus and Chaudhry (1994) using a depth-averaged k-ε model. In spite of the fact that their model accounted for viscous effects and turbulence, however, their predictions (when they minimized artificial dissipation in their model) were practically identical to the present results.

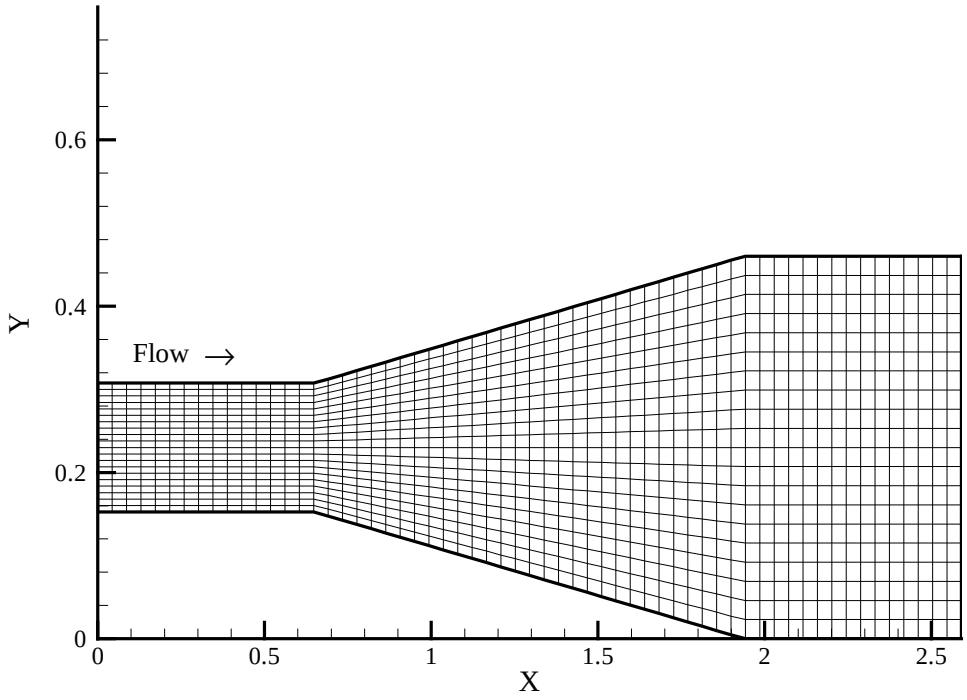

Figure 11. Grid and channel geometry for Case 4

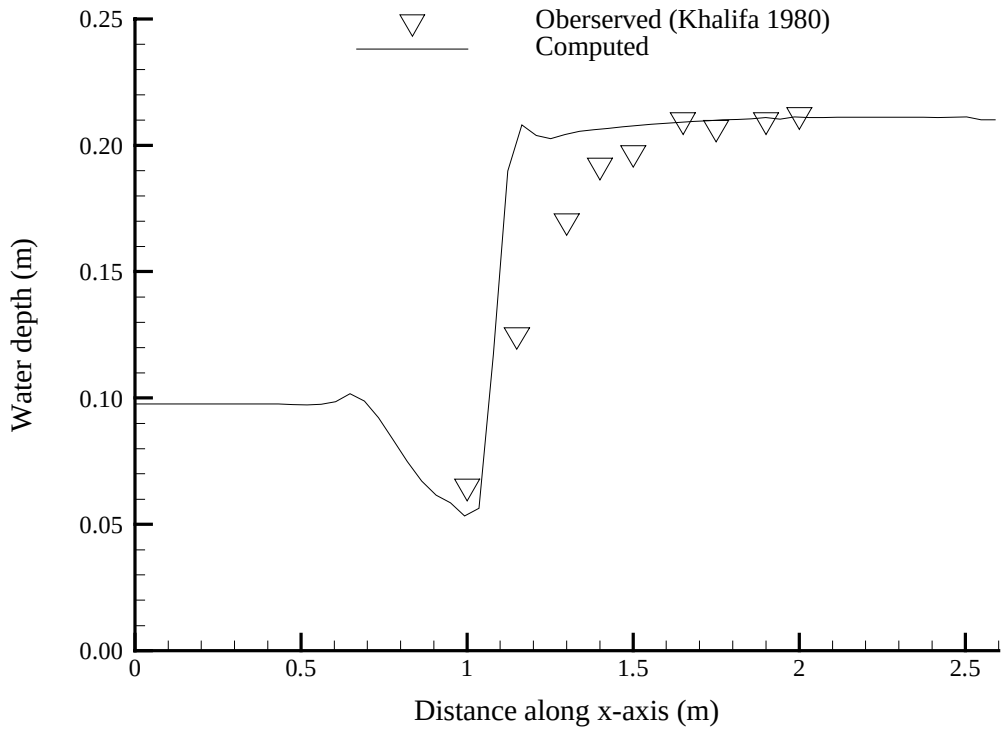

Figure 12. Comparison of 2D numerical model water surface profile with Khalifa (1980) experiment.

5. Conclusions and Future Research

We developed a two-dimensional, depth-averaged numerical model for simulating flows in natural river reaches. The model is formulated in generalized curvilinear coordinates so that the geometrical complexities of natural channels can be accurately resolved using body-fitted coordinates. Adaptive second- and third-order artificial dissipation terms are introduced to capture hydraulic jumps and ensure that accurate results can be obtained for all possible flow regimes. The discrete governing equations are integrated in time using a four-stage, second-order accurate Runge-Kutta time-stepping scheme. For steady-state computations, local time-stepping, implicit residual smoothing, and multigrid acceleration are used to enhance the efficiency of the numerical method.

The numerical model was validated by applying it to simulate a variety of open channel flows for which experimental data and numerical results have been reported in the literature. For all cases computed, the present method yielded results in good agreement with the measurements and previous numerical results from 2D and 3D models. Notable discrepancies between predictions and simulations were only observed for the strongly curved bend geometry. These discrepancies, however, should be attributed to the inability of the 2D model to account for three-dimensional effects and serve to illustrate the range of applicability of 2D models to channel geometries involving mild to moderate streamwise curvature. These discrepancies not withstanding, however, the comparisons with the data demonstrated that the present model is a powerful tool for accurate predictions of a variety of open-channel flow phenomena.

Due to the unavailability of necessary data, the numerical model could not be applied to the ACT and ACF basins as was originally intended. As we have already discussed, however, the model has been developed to be general enough so that it is readily applicable to natural channels. Application to river reaches in the ACT and ACF basins will require access to detailed bathymetry data and discharge and water-surface elevation measurements to be used for model calibration and validation. This objective will be pursued as part of future work.

6. References

Hu, S., and Kot, S. C. (1997), "Numerical model of tides in Pearl River estuary with moving boundary," ASCE J. Hydr. Eng. 123(1), pp. 21-29.

Jameson, A., Schmidt, W., and Turkel, E. (1981), "Numerical simulation of the Euler Equations by finite volume methods using Runge-Kutta time stepping schemes," *AIAA* paper 81-1259.

Jones, S. C. (1999) "Static mixers for water treatment: A computational fluid dynamics model," PhD thesis, Georgia Institute of Technology.

Khalifa, A. (1980), "Theoretical and experimental study of the radial hydraulics jump," Ph.D. dissertation, University of Windsor, Windsor, Ontario, Canada.

Kuipers, J., and Vreugdenhil, C. B. (1973), "Calculation of two-dimensional horizontal flow," Report S163, Part I, Delft Hydraulic Laboratory, Delft, The Netherlands.

Leschziner, Michael A. and Wolfgang Rodi (1979) "Calculation of strongly curved open channel flow," Journal of the Hydraulics Division, vol. 105, No. HY10, pp 1297-1314.

Lin, F., and Sotiropoulos, (1997) F., "Assessment of artificial dissipation models for 3-D incompressible flow solutions," *ASME J. Fluids Eng.* 119, 331-340.

McGuirc, J. J., and Rodi, W. (1978), "A depth-averaged mathematical model for the near field of side discharges into open-channel flow," *J. Fluid Mech*. 86(4), pp. 761-781.

Meselhe, E.A. and Sotiropoulos, F. (2000) "Three-dimensional numerical model for open-channels with free-surface variations." Journal of Hydraulic Research, vol. 38, pp 115-121.

Molls, T., and Chaudhry, M. H. (1995), "Depth-averaged open-channel flow model," *ASCE J. Hydr. Eng*. 121(6), pp. 453-465.

Muslim, M., and Spaulding, M. (1996), "Two-dimensional boundary-fitted circulation model in spherical coordinates," *ASCE J. Hydr. Eng*. 122(9), pp. 512-521.

Panagiotoopoulos, Alexander G. and Johannes V. Soulis (2000) "Implicit depth-averaged free-surface flow equations." Journal of Hydraulic Engineering, vol. 126, No. 6, pp 425-436.

Rastogi, A. K., and Rodi, W. (1978), "Predictions of heat and mass transfer in open channels," *ASCE J. Hydr. Div*. 104(3), pp. 397-419.

Rodi, W. (1980), "Turbulence models and their application in hydraulics," *IAHR monograph*, Delft, The Netherlands.

Rouse, H., Bhoota, V. V., and Hsu, E.-Y. (1951). "Design of channel expansions." Trans, ASCE, 116, 347-363.

Rozovskii, I. L., "Flow of water in bends of open channels," Israel program for Scientific Translation, Jerusalem, Israel, 1965.

Shankar, J., and Cheong, H.-F. (1996), "Boundary fitted grid models for tidal motions in singapore coastal waters," *IAHR J. Hydr. Res.* 35(1), pp. 3-19.

Tingsanchali, T., and Rodi, W. (1986), "Depth-averaged calculation of suspended sediment transport in rivers," 3rd Int. Symposium on River Sedimentation, The Univ. of Mississipi, March 31-April 4.

Turkel, Eli and Veer N. Vatsa (1994) "Effect of artificial viscosity on three-dimensional flow solutions," AIAA, vo1. 32, No. 1, pp39-45

Wenka, T., Valenta, P., and Rodi, W. (1991), "Depth-averaged calculation of flood flow in a river with irregular geometry," proc. of *XXIV IAHR Congress*, Madrid, Spain, Sept. 9-13, pp. A-225 to A-232.

Younus, Muhammad and M. Hanif Chaudhry (1994) "A depth-averaged $\hat{\kappa}-\hat{\varepsilon}$ turbulence model for the computation of free-surface flow." Journal of Hydraulic Research, vol. 32, No. 3, pp 415-444.

Basic Information

Title:	Sustainability of Surficial Aquifer Resources on Endmember (Urbanized and Pristine) Barrier Islands near Brunswick, Georgia
Project Number:	B-02-626
Start Date:	9/1/1998
End Date:	2/28/2001
Research Category:	Ground-water Flow and Transport
Focus Category:	Groundwater, Hydrogeochemistry, Solute Transport
Descriptors:	Geophysical methods, Saline intrusion, Island-estuary interface
Lead Institute:	Georgia Institute of Technology
Principal Investigators:	Carolyn Ruppel

Publication

1. Ruppel, C., G. Schultz, and S. Kruse, 2000, Anomalous freshwater lens morphology on a strip barrier island, Ground Water, 38, 872-881.
2. Schultz, G., and C. Ruppel, 2001, Independent constraints on hydraulic conductivity variations in a coastal surficial aquifer system, Ground Water, in review.
3. Schultz, G., and C. Ruppel, 2001, Frequency domain analysis of water table fluctuations in coastal aquifer systems, Water Resources Research, in review.
4. Schultz, G.M., and C. Ruppel, 1999, Independent constraints on hydraulic parameters and flow and transport in a coastal surficial aquifer system, EOS Transactions of the American Geophysical Union, 80(46), F422-423.

USGS-Water Resources Institute Program

Sustainability of Surficial Aquifer Resources on Endmember (Urbanized and Pristine) Barrier Islands near Brunswick, Georgia

Final Report

28 February, 2001

Dr. Carolyn Ruppel
Associate Professor of Geophysics
School of Earth and Atmopsheric Sciences
Georgia Tech
Atlanta, GA 30332-0340
cdr@piedmont.eas.gatech.edu
404 894-0231

Sustainability of Surficial Aquifer Resources on Endmember (Urbanized and Pristine) Barrier Islands near Brunswick, Georgia

Final Report

PI: Dr. Carolyn Ruppel, Associate Professor of Geophysics, Georgia Institute of Technology

Abstract

This report represents primarily a compilation of representative data obtained under the auspices of USGS-WRI funding between September 1998 and February 2001. The report covers the basics of the methods employed, the survey locations and raw results, the contributions to human resources, and the expected peer-reviewed publications that will acknowledge the award. Due to the volume of data obtained, this report focuses on only 3 issues: (a) regional hydrologic state of the two islands; (b) lateral saline intrusion at the island-estuary interface on the islands; and (c) redox zonation and groundwater geochemistry at a site with controlled anthropogenic inputs.

Introduction

The availability and quality of freshwater resources are key factors controlling the sustainability of natural systems (e.g., maritime forests, marshes, and migratory bird habitat) and human developments on barrier islands and the continued viability of ecosystems in adjacent wetlands and estuaries. One of the most important problems facing regional planners in coastal Georgia and, indeed, in most coastal areas of the world, is the impact of urbanization (increased population and industrialization), ecosystem destruction, and predicted sea level rise on the hydrologic systems of barrier islands. In North America, the Southeastern U.S. is unique in having a relatively high concentration of undeveloped barrier islands on both the Atlantic and Gulf Coasts. Economic pressure to increase tourism through urbanization of as-yet undeveloped islands and through continued urbanization of already heavily developed islands will continue to threaten the quality and quantity of freshwater in the surficial aquifer for decades to come.

The goal of this project was to apply the same geophysical and hydrologic methods to two islands in the Georgia Bight: a pristine island that can serve as the baseline for the undeveloped state and a developed island expected to undergo more urbanization in the coming years. As

interpretations of the results are still in progress, this report primarily focuses on presenting data collected under the auspices of USGS-Water Resource Institute sponsorship.

Geology

The islands of the South Atlantic Bight in Georgia (Figure 1) are mixed energy barrier beaches composed of Holocene and Pleistocene sediments [*Hayes*, 1994]. The islands' Atlantic coastlines are linear, have typical dune ridge morphology, and experience average tidal runup of several meters. Tidal creeks and sounds originate at the mouth of a major Southeastern river, the Altamaha and separate the landward side of the island from the mainland. These tidal creek systems influence the distribution of *Spartina* and *Juncus* marshlands along sides of the island not directly exposed to the ocean and play a critical role in flushing nutrients and other chemical constituents through estuaries. Tidal creeks and salt flats also separate the Pleistocene island core (landward side) from the Holocene accretionary complex (oceanward) [*Hayes*, 1994] on both islands (Figure 2). These tidal creeks provide drainage for large portions of the islands' interiors and represent a potential source of saline water input to the surficial aquifer of both the Holocene and Pleistocene sediment complexes.

Land Use

Sapelo Island

Of the barrier islands on the Georgia coast, Sapelo Island (Figure 3) is unique in being at once fairly pristine and fairly accessible. Despite past logging and the island's relatively modest area (<65 km^2), Sapelo Island is the site of 16% of the remaining maritime forest in the Southeastern U.S. [H. Hill, pers. comm., 1998]. The island's year-round population is ~70, mostly concentrated on the southern one-third of the island (Figure 4). A state-subsidized passenger ferry provides the only regular access, and only a few miles of paved roads are maintained for the island's residents. The island's weak economy is based on fishing and logging, but, as reported over the past several years by Atlanta's popular press, increased urbanization is strongly backed by the island's Gullah community, which views tourism as critical to solving the area's economic problems. Anecdotal evidence suggests that the number of people visiting the island each year has increased dramatically, possibly to over 15,000.

While many of these are day-only visitors, their use of septic systems and their reliance on pumping from the Floridan aquifer to meet drinking water and sanitation needs does mean an increased load on the island's resources. Both parts of this increased demand for resources will have an effect on the hydrologic state of the island. Greater demand for septic system capacity means the potential for greater contamination of the surficial aquifer and possible alterations to the levels of nutrients and the redox zones in the aquifer. Greater pumping of the deep aquifer means increased discharge of this water into septic systems and ultimately into the surficial aquifer. Eventually, the freshwater lens could undergo local thickening and the water table could shoal in some places due to anthropogenic processes.

St Simons Island

In sharp contrast to Sapelo Island, St. Simons Island (Figure 5) is a heavily urbanized island easily accessible via causeway to the mainland. The population of St. Simons fluctuates radically with the seasonal influx of tourists, and the island's proximity to Brunswick, Georgia and northern Florida has made it a desirable location for small businesses, vacation homes, and time-share condominium developments. The island's economy is integrally connected to tourism, and development of the island continues at a rapid pace. The island's drinking water supply is, like Sapelo's, pumped from the Floridan aquifer. In contrast to Sapelo, which relies exclusively on septic systems for management of wastewater, St Simons has an extensive sewer system. Thus, not all of the water pumped from the Floridan aquifer ends up in the freshwater lens. On the other hand, the concentration of golf courses on St Simons means that massive irrigation in some locations is greatly perturbing the local hydrologic cycle (e.g., Figure 6).

Methods

This study employs a suite of overlapping geophysical, hydrologic, and geochemical methods. This section provides a brief introduction to each technique.

Environmental geophysical methods

Remote sensing of subsurface geologic and hydrologic conditions using electromagnetic (EM), electrical, acoustic, and ground penetrating radar (GPR) methods represents a noninvasive, indirect approach to characterization of the shallow hydrology of barrier islands.

We acquire data using proven technologies (i.e., off-the-shelf equipment with known resolving power) applied along transects and in two-dimensional regions in the vicinity of important physical interfaces. While geophysical measurements can provide broad areal coverage, they are best at detecting *contrasts* in physical properties in the subsurface and at understanding a combination of lithologic, hydrologic, and saturation changes. Figure 7 shows the resolving power of geophysical methods relative to standard hydrologic methods. Geophysical techniques (Figure 8) provide an excellent means for noninvasive site characterization, but, even with advancements in instrumentation and inversion methods, geophysics will never provide information at the level of precision that discrete hydrologic measurements can.

Terrain conductivity measurements

The Geonics EM-31 and EM-34 constrain apparent conductivity to nominal depths of 6 m and 10-40 m, respectively, by measuring the ratio of the secondary to primary magnetic fields induced by introduction of a current (Figure 9). In the literature, EM methods have been widely applied in the mapping of saltwater intrusion, Dupuit-Ghyben-Herzberg lens morphology, and contaminant plumes. For this study, we use EM data to quantify changes in the depth to the water table and the form of the freshwater lens. When combined with electrical resistivity data, terrain conductivity data represent one of the most useful geophysical tools for characterization of surficial aquifers in barrier island settings.

DC Resistivity Measurements

DC resistivity methods also take advantage of differences in conductivity (inverse of resistivity) to map lateral and vertical variations in near-surface hydrologic and lithologic units. Small currents introduced into the ground through a pair of steel electrodes driven 6-8 inches deep produce a potential difference between a second pair of electrodes (Figure 9). Relating the applied current to the resulting potential difference through Ohm's Law (V=IR) permits the determination of electrical resistivity.

Ground penetrating radar

Ground penetrating radar (GPR) involves the introduction of radar waves directly into the ground through a transmitting antenna and reception of the returned signal through the receiving antenna. When implemented in bistatic mode (Figure 10), GPR operates on a principle similar to that of reflection seismology and provides an "image" of the uppermost meters of sediment (nominally 1 m to more than 10 m, depending on the frequency of the radar antenna). GPR is used to image subsurface geology, to constrain the top of high conductivity (saltwater) layers, and, in some cases, to locate the water table. The deep penetration of radar waves in unsaturated or freshwater saturated sandy sediments renders GPR far more useful than traditional acoustic (seismic) methods for constraining near-surface geologic structures that control flow pathways for the surficial aquifer. For sediments within tens of meters of the island-ocean or island-estuary interface on barrier islands, GPR is one of the best techniques for determining the location of the top of saltwater-saturated sediments.

Hydrologic Methods

Monitoring Well Network

This project partially supported expansion of our Sapelo Island monitoring well network, particularly at a site with known anthropogenic inputs (Moses Hammock). The purpose of the installation was to establish well networks for: (1) monitoring water levels and groundwater geochemistry, (2) mapping the local potentiometric surfaces; (3) determining hydraulic parameters of the surficial aquifer; and (4) quantifying the degree of interaction between the saline and freshwater at the boundaries of the island. In addition, the network provided valuable discrete hydrogeological and hydrogeochemical data that can then be used to support and groundtruth the geophysical methods.

This project assisted in supporting installation of 1.25 to 2.0" I.D. partially screened Schedule 40 PVC monitoring wells to depths of approximately 4.5 m (Figure 11). Wells were generally oriented along transects subperpendicular to the upland-estuary interface. The entire length of each well lies within the surficial aquifer, and local confining units (clay lenses) were encountered only during installation of wells 1 and 2 at Site 2. In these cases, the well point lies at the depth of the local, but not regional, confining units. To ensure minimal disruption to sediments and to groundwaters, wells were hand-augered through a 4.0" I.D. PVC cased hole. Each well was plugged and screened with 0.006-inch high-flow slots along the lowermost 2.5-5 ft. All regular monitoring wells used in

this study have fully saturated screen intervals under even the most severe drought conditions (e.g., late 1999 to present). After the well was in place in the borehole, well-sorted coarse (20-20 fill) silica filter pack was emplaced around the screen interval, and the 4.0" casing was removed. We then backfilled the borehole with natural fill and tamped the material around the well risers to prevent "bridging" and the formation of preferential conduits along the annular space. All wells were finished with a surface seal of quick-set concrete having a thickness of 4-8" and extending ~8-10" from the well on all sides. Manhole-cover style flush caps were used to finish the wells. Following installation, all wells were developed (pumped until clear), surveyed, and sampled.

Due to the largely private nature of land on St Simons Island, we realized early in this project that installing new environmental wells on the island would be impossible. Despite numerous contacts with coastal organizations that had access to private landowners with shallow wells, we were unable to obtain access to shallow groundwaters on St Simons Island. As we monitor the state of the island's surficial aquifer in the coming years, we are hopeful about eventually finding property owners willing to provide us with access to their private wells.

Water Level Monitoring

We monitored both static and dynamic water levels during this study. Static water levels were measured with a Solinst water level meter (both audible and visible level indicators) to an accuracy of 0.05" each time we visited the island. Dynamic water levels, or water levels during many tidal cycles, were occasionally logged every 10-30 minutes by specially constructed pressure transducers (2 to 5 psi full range) placed in the wells for periods as long as several weeks. More information about the analysis of these data was contained in Schultz (2000) and will be included in upcoming submissions (Schultz and Ruppel, 2001a, 2001b). The analysis of dynamic water levels provides critical information about such aquifer parameters as hydraulic conductivity.

Pumping Test

To provide information on the semi–instantaneous response of the aquifer, we conducted a short–duration pumping test using a 2" I.D. fully penetrating abstraction well at the Moses Hammock site. Water was extracted from MW0107 under water–table conditions at a constant rate of ~3.1 m^3 s^{-1} throughout the pumping portion of the experiment. During the pump and

recovery period, water levels were monitored with pressure transducers placed in two wells located within 3.0 m of the abstraction well. The results, shown in Figure 12, provide details about the hydraulic conductivity and storativity of the aquifer.

Groundwater Geochemistry

To constrain transport and the degree of interaction between saltwater and freshwater near the island-estuary interface, we conducted cation, anion, nutrient, and redox chemistry analyses of groundwaters and surface waters in the monitoring wells. This section details the methods used for the wellside analyses and the later laboratory analyses.

Water was sampled from the groundwater wells via peristaltic pump equipped with a 20 ft. section of hard poly-ethylene tubing. The tubing was extended the entire length of the well. Wells were pumped at high velocity when first opened to remove 5 L. This was done to purge the well of stagnant water and ensure sampling from the adjacent aquifer. The purged water was disposed and subsequent water was pumped into a plastic flow cell which contained three electrodes to measure pH, dissolved oxygen concentration, conductivity, temperature, and salinity. The top of the flow cell was the only portion open to the atmosphere. Well water was pumped into the bottom of the flow cell and allowed to pour over the top to prevent diffusion of gases from the atmosphere, specifically O_2, into the well water. The sensing part of the electrodes were placed in the bottom of the flow cell near the water input. Readings on all electrodes were allowed to equilibrate while water was flowing through the cell. This provided time for the electrodes to adapt to the various salinities present in the well field and further ensured water was being drawn from the aquifer providing sample integrity. A YSI – 55 DO meter was used to measure dissolved oxygen concentration, which were recorded in mg/L. A WTW combination pH, Conductivity, Temperature, and Salinity meter was used to measure these variables.

Samples were taken in 60 mL Becton-Dickson plastic syringes. A plastic adapter was fitted to the out end of the peristaltic pump tubing. This adapter ended in a two three-way stopcocks joined in series with luer-lock fitting on the ends. A two-way stopcock was attached to the end of the syringe and one of the ends of the final three-way stopcock. Well water was flushed through the two three-way stopcocks and then the final stopcock was turned to direct

flow into the syringe. The pressure of the pump filled the syringe. When the syringe was filled about halfway, the first stop cock was turned to divert the flow away from the syringe and final stopcock. The final stopcock was then turned to allow the syringe to vent out the end of the final stopcock. The syringe was oriented so that the outlet pointed straight up, forcing any gas bubbles to congregate at the opening. The syringe was then flushed. The procedure was reversed and the syringe was filled completely and the two-way stopcock turned to prevent flow from the full syringe. The syringe was disconnected and placed into a plastic bag continually overfilled with N_2 gas from a portable gas tank. The 'gas bag' was then put inside a cooler where it was kept cold and dark until analysis or preservation within 6 hours.

Iron and sulide analyses were conducted in the field with a Milton Roy UV/Vis Spectrophotometer and quartz cuvette. The syringes were taken from the 'gas bag' and a .45 um Whatman syringe tip filter with a luer-lock connection was attached to the end. Only enough sample (~ 5 ml) was filtered for the redox sensitive analysis (Fe, S) to save time. Fe was analyzed by a modification of the Stookey method and sulfide was measured by a modification of the Cline method. Once these analyses were completed, the remaining samples were filtered and divided into two equal aliquots (~ 25 mL) one of which was acidified and one of which was not. The acidified sample was used for cation analyses and the unacidified sample for anion analyses. All cations except Mn were analyzed on a Perkin Elmer flame AA, with acetylene as fuel. Mn was analyzed on a Varian graphite furnace AA with Zeeman correction. Cl and SO_4 were measured by spectrophotometric methods.

Depending on the species for which we were analyzing, samples were sometimes acidified within a few hours to prevent further reactions from occurring. At Georgia Tech, concentrations of key species were measured using atomic absorption (K^+, Al^{3+}, Ca^{2+}, Mg^{2+}, Fe_{tot} and Na^+) and spectrophotometric (Cl^-, NO_3^-, PO_4^{3-}, S^{2-}, NH_4^+, SiO_2, and alkalinity) methods. In general, the nutrient results (PO_4^{3-}, NO_3^-) results obtained using these techniques were unreliable. Nutrient analyses reported here were therefore completed on refrigerated groundwater samples by S. Joye (UGA) using an auto-analyzer. In general, Cl^- was difficult to interpret properly due to the high dilutions needed for the standards.

Representative Results

Here we report on representative results obtained as parts of this study. No attempt is made to provide an exhaustive compilation of our data or results, since we anticipate peer-reviewed publication of much of this research. We also do not provide detailed interpretations in this report. We have chosen to present results focused on three different areas: (a) the regional hydrologic state; (b) local saline intrusion at the island-estuary interface; (c) redox zonation at a site with controlled anthropogenic input from a shallow septic tank system.

Regional Hydrologic State

A key goal of this project was to characterize the regional hydrologic state of the two islands using remote sensing (geophysical) data. We used primarily inversions of EM-34 and EM-31 data to achieve this goal. As noted earlier, EM-34 and EM-31 data provide the integrated terrain conductivity in the upper part of the sedimentary section and are particularly useful at delineating the location of high and low conductivity pore waters. The theory underlying EM-34 and EM-31 data interpretation relies on a linear relationship between the primary magnetic field produced by the instrument's alternating current and the secondary magnetic field that arises due to induced eddy currents. The multiplicative (linear) factor should represent the Earth's conductivity. However, the technique breaks down at high induction numbers, which are characteristic of high conductivity terrains. Thus, collected data must be corrected for nonlinear effects associated with the presence of high conductivity material pore waters within the sensing depth of the instrument. These nonlinear effects are shown in Figure 13 for the horizontal dipole orientation. Even with the correction for the nonlinear effect, there are still known difficulties with use of standard inversion techniques in high conductivity terrains. We here interpret the interface depth as a discrete boundary, although, in real systems, a dispersive transition zone separates the fresh water from the underlying saline water. Geophysical data cannot resolve such fine-scale features without the application of much more advanced inversion techniques.

Sapelo Island

This project sponsored the acquisition of a full cross-island EM-34 transect on Sapelo Island. These data supplement those acquired exclusively at the edges of the island several years ago. The new, corrected data, collected at the location shown in Figure 3, are shown in Figure 15. These data are highly complicated at the edges of the island, and further analysis of

nonlinear effects at these locations will be necessary. In the center of the island, the very low terrain conductivity values probably constrain the depth of the water table (unsaturated-saturated interface) more than the depth to the base of the saltwater lens. To first order, though, the data in Figure 15 can be interpreted

We also have an older composite result that constrains the morphology of the freshwater lens. These results, shown in Figure 16, indicate a normal lens morphology, with the thickest part of the lens near the estuary (eastern) side of the island, as would be expected from simple theory. For this profile, we had no data in the center of the island, though, and thus could not constrain the lens thickness there.

We also acquired 50 MHz, bistatic-mode GPR images across the island to constrain subsurface hydrologic structure for comparison with St Simons Island. The results, shown in Figure 16, highlight the variable thickness of the freshwater lens across the island at the location shown in Figure 3. Because radar waves are highly attenuated by saline waters, the base of the lens roughly corresponds to the region that is "blanked" in the profile. The accretionary structure of the island, which may provide some control on flow pathways, is manifested here as steeply dipping sediments within the freshwater zone. Note that the water table does not lie completely flat. The road on either side of this transect has been canalized in some places. Given the interaction of the water table with these surface water bodies, it is not surprising that the water table seems to have greater variation than would be expected for the very flat topography and highly homogeneous sediments of the area.

St Simons Island

Due to problems with electrical utilities and lack of undeveloped transects in other parts of the island, we completed as much of a cross-island survey as possible on the north part of St Simons Island within a tract of land owned by the Sea Island Company. The transect, whose location is shown in Figure 5, ran nearly due west, starting at the island-tidal creek interface. We were unable to find a location at which we could complete the transect on the ocean side of the island. Raw EM-34 data collected along the transect are shown in Figure 18. The area in which we conducted the EM-34 survey could eventually be developed by the Sea Island Company. Thus, we anticipate that re-occupation of the survey sites at other times may help us to document

the impact of both natural (e.g., drought) and anthropogenic (e.g., due to possible construction) on this area.

We also collected a cross-island GPR survey at the Sea Island Company site. The unprocessed data, shown in Figure 19, bear a striking similarity to those obtained on Sapelo Island (Figure 16). An important similarity between the profiles is the presence of a strong reflector at the apparent top of the saline water zone at the island-estuary side of the profiles. In theory, we would not expect such a reflection, and the precise origin of this feature remains unknown. Note the fluctuations in the water table in Figure 19 (~50 ns TWTT) and the change in the character of the section at ~1000 m, near the location of the freshwater wetlands.

Comparison with Gulf Coast barrier island

The results can be compared to those described in Ruppel et al. (2000) for a developed barrier island on the Florida Gulf coast. In that study, the morphology of the freshwater lens on a thin (< 1 km wide) barrier island with an enclosed estuary (Apalachicola Bay) on the north side was shown to be asymmetric, but with a morphology different from that usually associated with barrier islands. Those results, shown in Figure 20, may be indicative of higher mean sea level on the bay side of this island than on the ocean side. Such a pattern of sea level differences would produce a thicker lens adjacent to the ocean side of the island. For Sapelo and St Simons, the large tidal range on the Atlantic coast relative to that in the estuary and the fact that the coastal rivers discharge not into enclosed bays, but rather into sounds between the islands, implies that EMSL is likely higher on the ocean side. This would be consistent with the formation of a freshwater lens with a normal sense of asymmetry (skewed toward the estuary).

Saline Water Intrusion at the Island-Estuary Boundary

Due to the ecologically-sensitive nature of estuaries, the propensity of developers to build close to the island-estuary boundary, and the proximity of so many coastal septic systems to the estuary side of the state's barrier islands, hydrologic processes at the island-estuary boundary and within the upland adjacent to estuaries are of critical importance to the study of development-related issues in coastal Georgia. In this study, we conducted intensive surveys at the island-estuary boundary on both Sapelo and St Simons Islands.

Sapelo Island

This project provided partial support for the acquisition of multinode DC resistivity data and inductive EM data at Moses Hammock, the controlled anthropogenic input site on Sapelo Island. As noted earlier, Moses Hammock is surrounded by salt marsh, and, to a large extent, the island can serve as a microcosm for the larger island to which it is adjacent.

Figure 21 shows pseudo-sections of multinode DC resistivity data taken parallel to the tidal creek at the Moses Hammock site. These results reveal the subsurface distribution of fresh and saline water beneath the eastern edge of Moses Hammock and imply that lateral intrusion of saline water at this site exceeds 30 m. These results have been verified by acquisition of conductivity readings in monitoring wells and major ion analyses of groundwater samples. (See geochemistry section).

We contrast these results with those obtained at a low salinity site instrumented primarily under the auspices of our NOAA-sponsored research. The Kenan Field site, which is adjacent to a smaller tidal creek that has a much more vertical creek bank, has lateral saline water intrusion of less than a few meters (Figure 22). Once again, these results have been verified by conductivity logging and major ion analyses.

During the course of this project, concurrent research, and previous projects, we also repeatedly measured terrain conductivity at the upland-estuary interface at Moses Hammock in an attempt to tie the results to the changes in recharge rates. The only water source on the hammock is pumping from the Floridan aquifer. The aquifer is pumped at most a few hours a day during the few weeks each year when the hammock is used as a hunt camp. Therefore, any overall effects in the freshwater budget beneath the hammock can be largely attributed to changes in recharge. Figure 23 shows the correlation between degree of saline water intrusion (cast as conductivity variations) and precipitation records. The lateral extent of saline water intrusion does not vary appreciably, but the slope of the leading edge of the freshwater interface does change. Thus, we view the absolute lateral extent of saline water intrusion as largely static (steady-state), while the thickness and size of the freshwater lens changes with time.

St Simons Island

On St Simons Island, we conducted surveys at the island-estuary interface at the site of the Sea Island company transect and at two locations within the Fort Frederica National Monument. The sites at Fort Frederica were reoccupied at distinct times about one year apart, using the same technique but different equipment. The Sea Island Company transect was occupied only a single time, in December 2000. Survey locations are shown in Figure 5.

Figure 24 shows pseudo-sections obtained at the north and south transects at the Fort Frederica site in 1999. Here we note a significant contrast in the inferred degree of saline water intrusion at two sites separated by only a few hundred meters. The northern site has lower elevation (plot not shown here) and is adjacent to a small creek flooded at spring tide. Saline water at that location exceeds 30 m. At the southern site, in a stand of live oaks adjacent to a steeper bank and on higher elevation upland sediments, saline intrusion is limited to < 10 m. In December 2000, we collected new DC resistivity data along the same survey lines. For these surveys, we used a multinode automatic switching resistivity system operated in dipole-dipole mode. The pseudo-sections, shown in Figures 25 and 26, resolve the subsurface structure much better than those compiled with data collected with traditional dipole-dipole surveys. A multinode resistivity survey at the island-estuary interface along the Sea Island Company transect was also characterized by a low degree of saline water intrusion, as demonstrated in Figure 27.

We collected coincident terrain conductivity data at both the Fort Frederica and the Sea Island Company survey sites. These data suffer from significant difficulties associated with the nonlinearities caused by the presence of saline waters in the shallow subsurface. The resulting two-layer inversions for the Fort Frederica data are shown in Figures 28 and 29. Note the rough correspondence between the presumed thickness of the freshwater lens from these data and from the dipole-dipole resistivity data.

We also acquired GPR data along the Fort Frederica transects. The results, shown in Figures 30 and 31, provide greater control over hydrofacies. Note that the water table varies gently along these profiles and that a deeper reflector possibly associated with a fresh-saline water boundary is once again visible.

Factors Contributing to Saline Water Intrusion in the Surficial Aquifer

To first order, three primary factors seem to contribute to the degree of lateral saline intrusion into the surficial aquifer at the upland-estuary interface. These factors are (1) elevation of the site relative to the surrounding marsh and mean tidal creek water depth, (2) morphology of the creek bank, and (3) order of the tidal creek.

The elevation effect is clearly demonstrated at the Fort Frederica site, where one side of the site (south) is at higher elevation than the other (north). The DC resistivity data show greater intrusion at the northern site than at the southern. The elevation effect primarily reflects the closer proximity of the top of the saline water at the northern site. However, this site is also slightly contaminated by a 3D effect due to saline water flooding the intermittent creek adjacent to the northern side of the transect. Part of the lateral intrusion inferred at this site may be related to a saline signal in the pore waters due to the last flooding of that creek.

The morphology effect is most clearly demonstrated by comparing the Moses Hammock site to the Kenan Field site on Sapelo Island. The morphology of the bank at the Moses Hammock site is complicated and departs significantly from the idealized vertical boundary condition associated with tidal creek banks adjacent to the upland on some parts of the barrier islands. The Duplin River, a major tidal river exactly analogous to Frederica River on St Simons Island, lies tens of meters from the edge of the upland at Moses Hammock. The intervening marsh and small levee system completely floods only at high high tides and spring tide. In contrast, the Kenan field site lies adjacent to a nearly vertical tidal creek bank. The results from Kenan Field show only a small degree of lateral saline water intrusion. Ironically, flat, marshlike creek banks seem to encourage lateral intrusion of saline water more than vertical creek banks. This may be related to the longer periods of flooding and greater infiltration times for saline water on flat creek banks. Alternately, clogging of the aquifer near the estuary may act as a physical barrier to saline water penetration, and such clogging may be greater at vertical creek banks that truly act to 'contain' the river at high tide than at more gently sloping banks that are merely flooded at high tide. We have preliminary evidence that clogging is an important factor in preventing saline water intrusion at the Kenan Field site relative to the Moses Hammock site on Sapelo Island. (Schultz and Ruppel, in prep, 2001a).

The final effect may be related to the order of the tidal creek. The Duplin and Frederica rivers are the major tidal systems on the estuary side of Sapelo and St Simons Islands, respectively. These rivers are swift and wide with well-established channels. Barn Creek,

which lies adjacent to the Kenan Field site, and the smaller creek adjacent to the island-estuary site along the Sea Island Company transect, are tributaries of the major tidal rivers. Smaller creeks further removed from the major tidal creeks tend to have lower salinity. Thus, even if these creeks did intrude into the upland, we may have a more difficult time detecting the entire signal related to that intrusion.

Groundwater Geochemistry

Redox Chemistry

In the course of this experiment, we have heavily instrumented a self-contained freshwater system on Moses Hammock on Sapelo Island. As noted earlier, the site, shown in Figure 3, has sporadic human habitation during the deer hunting season. Waste is dealt with through a septic system, and the only running water is pumped from the deep Floridan aquifer for at most several hours per day for very brief periods during the hunt season. To first order, this system represents a perfect microcosm for studying the groundwater chemistry associated with saline-freshwater interactions in the subsurface. At a secondary level, this site permits an examination of the direct impacts of human habitation on a well-defined and confined site.

The geochemical analyses on groundwaters at the Moses Hammock site were conducted on samples taken from the monitoring well transects. The most important result to emerge from the redox analyses is the existence of multiple redox fronts in the surficial aquifer. Figure 31 shows Fe(II) and Mn (II) concentrations across Moses Hammock and reveals the existence of an expected diagenetic pattern within the aquifer on both sides of the hammock. This diagenetic "front" is symmetric on both sides of the hammock and correlated with the location at which the saline waters encounter fresh waters.

However, the surficial aquifer appears to contain a superposed set of redox zones at this site. Within the small freshwater lens, a second Fe(II) to Mn(II) front appears. In effect, this second zone may be the normal one expected within the freshwater aquifer. The more anomalous redox front may be the first one encountered with increasing distance from each side of the hammock. This redox front seems to be correlated with the region of highest salinity

gradient. We are continuing to build a time series of spring tide geochemical measurements to further refine these relationships.

Nutrient Analyses

As part of this project, colleague S. Joye at UGA conducted nutrient analyses on groundwater and surface water samples at our well sites. The original goal of this work was a comparative study with the nutrient dynamics on St Simons. Without well waters from that location, a one-to-one comparison of nutrient levels was not possible. However, limited nutrient data available from the surface waters near St Simons (Georgia LMER project) can be used to compare at least the estuary components of these two systems.

Figure 32 shows a compilation of nutrient levels at the Sapelo well sites and in adjacent surface waters (Hunter et al., 2000). The most striking trend to emerge from these analyses is the very low nutrient levels within the island proper. In fact, slightly elevated levels of nutrients are observed only immediately adjacent to the estuary and usually at values quite similar to those in the adjacent estuary waters. This implies that nutrients are mostly coming from the waters that infiltrate the surficial aquifer, not being derived on the island itself.

Major Ion Analyses

We have conducted several complete major cation and anion analyses of groundwaters at the Sapelo Island well sites. Such data are primarily used to verify our geophysical inferences about the distribution of fresh and saline waters and to conduct mixing calculations to determine the balance of rainwater (recharge), foreign water (Floridan aquifer), and creek water in the freshwater and saltwater systems beneath various parts of the study area. Only two representative results are provided here (Figures 33 and 34) as an example of the data that have been collected and for comparison with the DC resistivity results shown earlier.

GIS

In the course of this project, we have developed extensive GIS for both Sapelo and St Simons Island. Eventually, we hope to integrate hydrologic analyses of the regional databases (e.g., using Maidment's analysis tools) with the interpretations gleaned from our local surveys. GIS-based maps derived from our new products are shown in Figures 3-6 of this report.

Contribution to Human Resource Development

This project has contributed to the M.S. thesis of Matthew Snyder (expected August 2001), to the Ph.D. work of Greg Schultz (expected early 2002), and to the B.S. level training of a host of undergraduate researchers, including B. Robinson, P. Fulton, S. Scharf, A. Hutko, and T. Garner. A. Hutko is now in a geophysics Ph.D. program at Scripps Institute of Oceanography. T. Garner currently works at Skidaway Institute of Oceanography. S. Scharf has been offered a job by Schlumberger Oilfield Services based primarily on his experiences with this project. B. Robinson is currently teaching environmental science in China as a Peace Corps volunteer. P. Fulton continues to work on various hydrologic projects in our lab and will be completing research with us during Summer 2001. Matthew Snyder's MS work focuses on redox zonation of the groundwater at the Moses Hammock site. Greg Schultz's PhD work focuses on a variety of geophysical and hydrological topics related to groundwater flow in the coastal zone.

The project has partially supported the presentation of our results to a number of professional forums and has been appropriately acknowledged in at least 3 or 4 oral or poster presentations. In addition, the project contributed to a research-based undergraduate course by providing some of the infrastructure for the students' analyses of water resources in their coastal zone field area.

Expected Outcomes

As we complete interpretation and synthesis of our data in the coming months, we anticipate the following products:

- Snyder MS thesis and related submissions to peer-reviewed journals
- Submission of Schultz and Ruppel (2001a, 2001b)
- Completion of a comparative manuscript on St Simons and Sapelo Islands

In the future, we plan to reoccupy the long transect on St Simons Island, particularly if the Sea Island company develops this land. We have learned that completion of new geophysical surveys at formerly occupied sites often provides invaluable information about the impact of natural and anthropogenic inputs on the system.

References

Ruppel, C., G. Schultz, and S. Kruse, Anomalous freshwater lens morphology on a strip barrier island, *Ground Water*, *38*, 872-881, 2000.

Schultz, G., Independent constraints on hydraulic conductivity variations and transient flow in a coastal surficial aquifer system, qualifying exam paper, Georgia Institute of Technology, 2000.

Schultz, G. and C. Ruppel, Geophysical and hydrologic characterization of spatial and temporal variations in the distribution of freshwater and saltwater at the island-estuary interface, Sapelo Island National Estuarine Research Reserve, *NOAA-NERRS Final Report*, 113 pp., October, 2000.

Schultz, G. and C. Ruppel, Independent constraints on hydraulic conductivity variations in a coastal surficial aquifer system, in preparation for *Ground Water*, submission expected Spring 2001, early 2001a.

Schultz, G. and C. Ruppel, Frequency domain analysis of water table fluctuations in coastal aquifer systems, in preparation for *Water Resources Research*, submission expected Spring 2001, 2001b.

Selected Presentations Acknowledging WRI support

1. Schultz, G. and C. Ruppel, Groundwater flow and salt transport at the island-estuary interface, Long Term Ecological Research annual meeting, August 2000.
2. Schultz, G. and C. Ruppel (invited), Integrated application of non-invasive geophysical and hydrologic methods for coastal aquifer characterization, Georgia Ground Water Association, May 2000.
3. Hunter, K.S., Lee, R.Y., Boyd, B., Schultz, G., Joye, S.B., and Ruppel, C., Groundwater geochemistry at the island-estuary interface at perturbed and pristine sites on a Georgia Bight barrier island, Southeastern Section, Geol. Soc. Amer., Annual Mtg., 2000.
4. Schultz, G.M. and C. Ruppel, Independent constraints on hydraulic parameters and flow and transport in a coastal surficial aquifer system, *EOS Trans. Amer. Geophys. Union, 80(46)*, F422-423, 1999.

The figures have been omitted from this project report for purposes of uploading to the NIWR.org system. Those wishing to obtain the report figures may contact Dr. Ruppel using the contact data provided on the cover page or may contact the Georgia Water Resources Institute.

Basic Information

Title:	Improvement to Water Resources Management Due to Climate Forecasts
Project Number:	E-20-640
Start Date:	8/1/1997
End Date:	12/31/2000
Research Category:	Climate and Hydrologic Processes
Focus Category:	Climatological Processes, Hydrology, Management and Planning
Descriptors:	Climate forecasts, Decision support system, Hydrologic modeling, Reservoir operation
Lead Institute:	Georgia Water Resources Institute
Principal Investigators:	Aris Peter Georgakakos

Publication

1. Georgakakos, A., and H. Yao. 2001. "Assessment of Folsom Lake Response, 2, Reservoir Management." Journal of Hydrology. in press.
2. Georgakakos, K.P., A.P. Georgakakos, and N.E.Graham. 1998. "Assessment of Benefits of Climate Forecasts for Reservoir Management in the GCIP Region." GEWEX News, 8(3), pp. 5-7.
3. Georgakakos, A.P., H. Yao, M.G. Mullusky, and K.P. Georgakakos. 1998. "Impacts of CLimate Variability on the Operational Forecast and Management of the Upper Des Moines River Basin." Water Resources Research, 34(4).
4. Georgakakos, A.P., H. Yao, T.M. Carpenter, and K.P. Georgakakos. 2001. "Value of Climate Forecasts for Lake Saylorville and Lake Lanier." Journal of Geophysical Research. (in preparation).

PROJECT SUMMARY

The focus of this three-year project was to quantitatively assess benefits that use of climate information and forecasts has for the improved management of reservoir hydrosystems. The project was a collaboration of a climate and hydrologic forecast group (HRC/SIO), and a reservoir decision support group (GIT). The primary tool for quantifying the benefits is a numerical system, which includes components for generating *(a)* hydrologic forecasts and forecast uncertainty estimates through ensemble forecasting conditional on GCM information, and *(b)* trade-offs for decision support of multi-objective reservoir operation at a given level of reliability. Quantiles of the distribution of climate-model precipitation simulations are used to select catchment-scale historical daily precipitation time series for the generation of an ensemble of daily reservoir-inflow by hydrologic models. Retrospective studies involving historical multi-decadal climate, hydrologic and reservoir-operation data, together with a variety of scenarios of climate information were performed for the assessment of benefits. The research was performed in collaboration with management authorities and forecast agencies. Saylorville Lake on the Upper Des Moines River in the Midwestern U.S., operated by the U.S. Corps of Engineers, and Lake Lanier on the Chattahoochee River in Georgia operated by Georgia Power, constituted the case studies for this work. Forecast methods suitable for implementation in real time were also developed for the Panama Canal Watershed, where the ENSO signal is strong.

The following are important lessons learned from this study:

- Utilization of climate information for reservoir management is best accomplished through integrated forecast-control systems with a consistent flow of the significant forecast and management uncertainties through the system components and with the ability to translate improved forecast skill to improved quantitative reservoir management benefits.
- Perhaps more than other components, explicit modeling of uncertainty by the forecast and decision systems is a necessary prerequisite for utilizing uncertain

climate forecast information by reservoir systems. Reliability measures of ensemble forecast validation are appropriate in this framework.

- GCM forecasts must be combined with available historical records for their profitable utilization on the scales of drainage catchments, which provide reservoir inflow. This research contributed toward the development of probabilistic diagnostic measures for climate model information for hydrologic and water resources applications.
- Decision support systems must be dynamic and tailored to each application. There is great leverage against erroneous forecasts that can be had with well designed such systems.
- Designing and building successful integrated end-to-end forecast-control systems must involve reservoir engineers, operators, and managers together with forecast scientists and modelers.
- Climate model forecasts and simulations improved economic reservoir management performance over the use of historical climate information for historical extreme high flow cases at the Midwestern Saylorville reservoir. The large storage capacity of Lake Lanier and its ability to release significant volumes of water without significant damage downstream are responsible for the lack of significant benefits from using climate-model over historical climatological information.

Refereed publications produced from this research are listed below:

Georgakakos, K.P., A.P. Georgakakos and N.E. Graham, 1998: "Assessment of Benefits of Climate Forecasts for Reservoir Management in the GCIP Region," *GEWEX News*, **8 (3)**, 5-7.

Georgakakos, A.P., H. Yao, M.G. Mullusky, and K.P. Georgakakos, 1998: "Impacts of Climate Variability on the Operational Forecast and Management of the Upper Des Moines River Basin", *Water Resources Research*, Vol. **34(4)**.

Georgakakos, K.P., 1998: "Flooding Attributable to El Nino," *World Meteorological Organization Bulletin*, **47(4)**, 356-360.

Georgakakos, K.P., 2001: "Probabilistic Climate Model Diagnostics for Hydrologic and Water Resources Impacts Studies," *Bulletin of the AMS*, **(in preparation)**.

Carpenter, T.M., and Georgakakos, K.P., 2001: "Ensemble Hydrologic Forecasting with Global Climate Model Information for Water Resources Management," *J. Hydrology*, **(in preparation)**.

Georgakakos, A.P., Yao, H., Carpenter, T.M., and K.P. Georgakakos, 2001: "Value of Climate Forecasts for Lake Saylorville and Lake Lanier," *J. Geophysical Research*, **(in preparation)**.

Basic Information

Title:	Climate and Hydrologic Forecasts for Operational Water Resources Management
Project Number:	E-20-F21
Start Date:	9/1/1999
End Date:	8/31/2002
Research Category:	Climate and Hydrologic Processes
Focus Category:	Management and Planning, Climatological Processes, Water Quantity
Descriptors:	Climate forecasts, Decision support system, Hydrologic modeling, Optimized multipurpose reservoir operation, Global circulation models
Lead Institute:	Georgia Water Resources Institute
Principal Investigators:	Aris Peter Georgakakos

Publication

Progress Report

"Climate and Hydrologic Forecasts for Operational Water Resources Management: A Demonstration Project"

NOAA Grant NA96GP0408 (Award Period: 1 September 1999 to 31 August 2002)

Principle Investigators: **Aris Georgakakos**
Georgia Water Resources Institute / Georgia Tech
and
Konstantine Georgakakos
Hydrologic Research Center / Scripps Institution of Oceanography

A. Activities of the Georgia Water Resources Institute (GWRI)

During the first project period, the Georgia Water Resources Institute worked on developing the background data and modeling elements for the Lake Norris demonstration project. The principal elements of the assessment framework are shown on Figure 1 and include (a) climate/hydrologic forecasting, (b) reservoir management, and (c) scenario assessment. The climate/hydrologic forecasting task for Lake Norris is undertaken by the Hydrologic Research Center (HRC) and is discussed in Section B of the report. Reservoir management is based on a decision system that includes three coupled models pertinent to turbine commitment and load dispatching, short/mid-term energy generation scheduling (hourly time steps), and long-term reservoir management (weekly time steps). The purpose of the scenario assessment element is to measure the benefit of using climate information within the integrated forecast-control process by replicating the system response under the guidance of the decision system.

Lake Norris data were obtained by TVA and used to develop the turbine commitment and load dispatching (TC&LD) and short-term energy generation models. The purpose of the TC&LD) model is to optimize hydro plant efficiency by determining the power load of each turbine such that a certain power level (for the entire plant) is generated at minimum discharge. This model requires the following inputs:

- beginning-of-the-period reservoir elevations;
- various turbine and reservoir characteristics (e.g., elevation vs. storage and tailwater vs. discharge relationships, power vs. net hydraulic head vs. discharge curves, and operational turbine ranges, among others);
- turbine outage schedule; and
- minimum and maximum discharge requirements.

The optimization problem associated with the TC&LD model is solved via Dynamic Programming and provides the maximum possible power associated with a particular discharge level, or (equivalently) the minimum discharge that achieves a particular power level. The role of the model is (**1**) to develop (off-line) the optimal (best efficiency) relationship among total outflow, total power generation, and reservoir elevation for each power plant, and (**2**) to determine (in an operational mode) the actual turbine loads that realize the discharge assigned to a particular plant from the upper level models. The first output is the connecting link between this and the short/mid-term energy generation model.

The first purpose of the short/mid-term model is to derive a near-optimal function among reservoir level, weekly release volume, and energy generation to be used by the long range

control model. For a particular reservoir level and a weekly release volume, this relationship is obtained by determining the hourly plant releases that sum up to the given weekly volume and maximize energy generation. The complete function is developed by performing this off-line computation for various combinations of reservoir level and weekly release volume. This model requires the following inputs:

- the optimal level-discharge-power curve derived by the previous model;
- feasible reservoir level ranges; and
- minimum and maximum discharge requirements.

The second purpose of the short/mid-term model is to operationalize the weekly decisions of the long-term model by generating hourly release and energy generation schedules. The optimization process for this model is also carried out using dynamic programming.

Both models have been developed and are currently being tested for a variety of hydrologic and operational conditions. This process is scheduled for completion by the end of the first project phase (August 31, 2000). The second and third project phases will be dedicated to the development of the remaining models and the performance of the assessment investigations.

B. Activities of the Hydrologic Research Center

(Supported through a sub-contract to GWRI)

During the first project period, Hydrologic Research Center Staff in collaboration with regional National Weather Service Staff estimated the parameters of the operational Sacramento soil moisture accounting and channel routing model for both the 3,817-km^2 Clinch River at Tazewell, TN, and 1,774-km^2 Powell River at Cleveland, TN. Parameter estimation was accomplished using the methods and techniques described in NOAA-HRC (1999) using a quality-controlled database of daily data (precipitation, temperature, pan evaporation). (The database was developed as part of this project.) The Clinch and Powell Rivers provide the inflow to Lake Norris. Operational forecast models were used to allow the assessment of the value of climate information for the Lake Norris reservoir management in an operational environment.

The results of parameter estimation for the two Rivers are summarized in Figures HRC-1 and HRC-2. No significant biases exist in reproducing the annual cycle of monthly-averaged daily flows, and the variability of the flows, as indicated by the standard deviation of daily flows in each month, is reasonably well reproduced throughout the year. Slight underestimation of daily flow variability is observed for most of the winter and spring months for both catchments. The cross-correlation of daily observed and simulated flow for both catchments is about 0.9, which implies that the operational forecast model, running in simulation mode, explains approximately 80 percent of the observed daily flow variance.

For the remaining period of the first year of the project, we will develop baseline ensemble streamflow forecasts incorporating the uncertainty in precipitation and potential evapotranspiration forcing and model errors. We will validate such ensemble forecasts using reliability plots and scores (Carpenter and Georgakakos, 2000) and will provide such ensemble forecasts to the Georgia Tech team to produce quantify the benefits due to reservoir management resulting from such forecasts. These would be compared to simple regression forecasts that resemble the current operational forecasts used for the operational management of Lake Norris.

During the second year of the project we will use forecasts of global climate models (Canadian CGCM1 and ECHAM3) to condition the ensemble streamflow forecasts to allow evaluation of the value of climate information for the management of Lake Norris. Analysis of the reliability of the climate information for the region will also be performed.

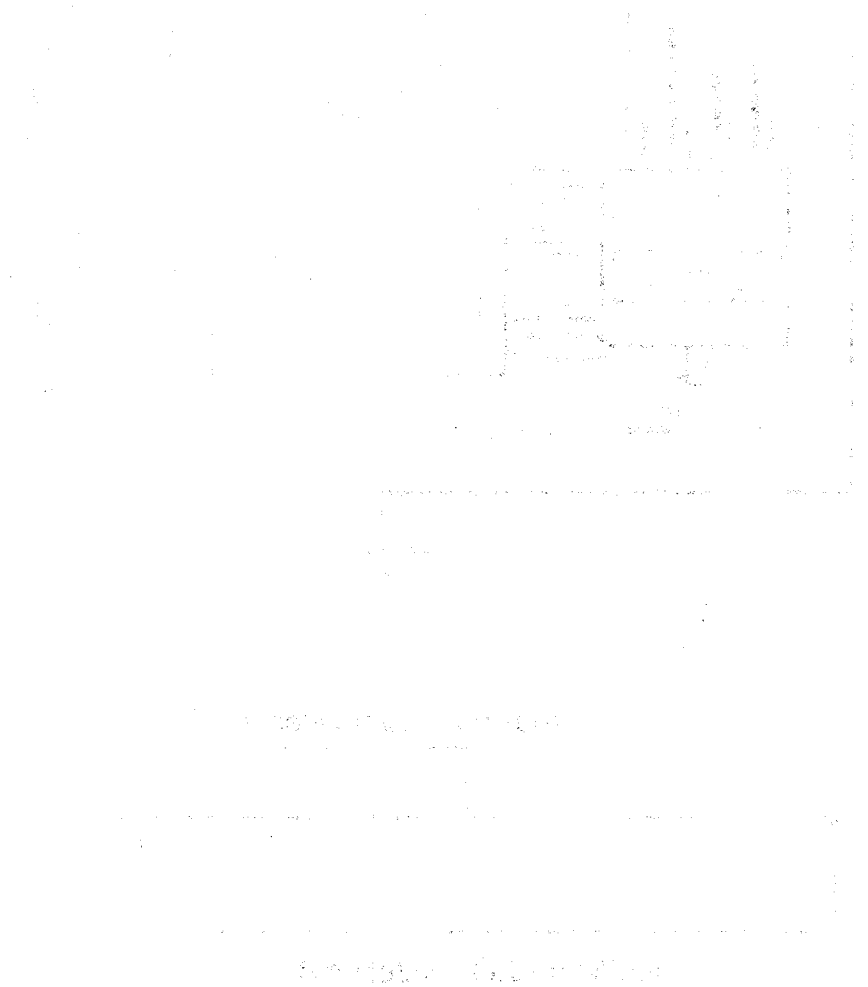

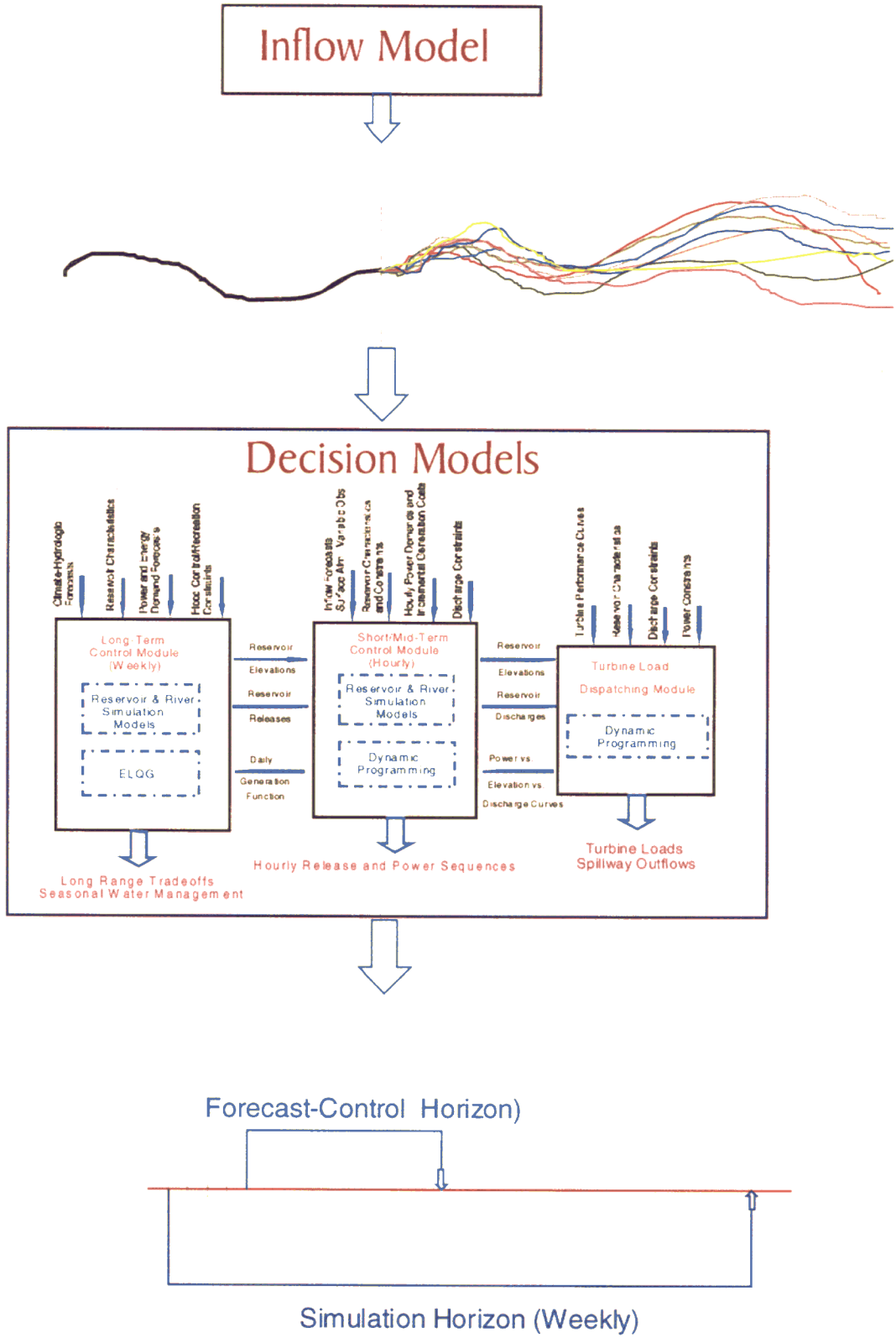

Figure GWRI-1: Modeling Framework and Assessment Process

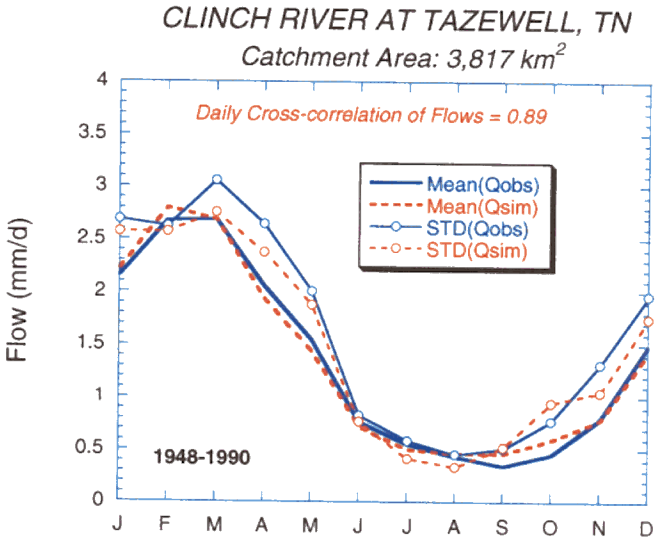

Figure HRC-1. Performance measures for Clinch River catchment for period 1/1/1948-12/31/1990.

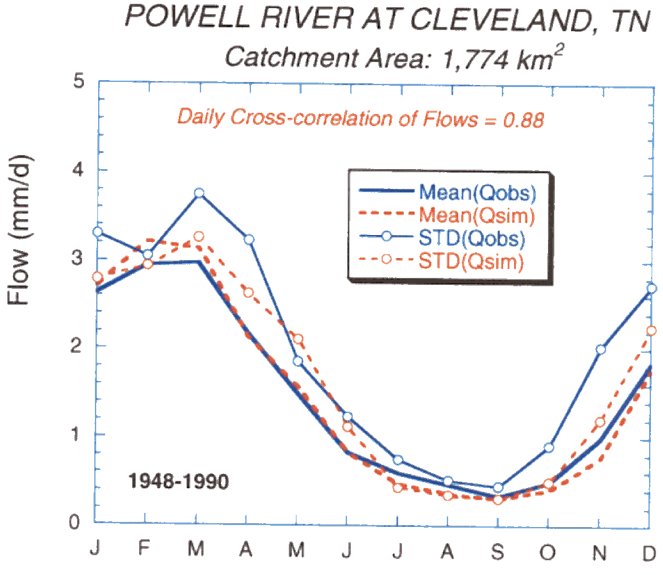

Figure HRC-2. Performance measures for Powell River catchment for the period 1/1/1948-12/31/1990.

Basic Information

Title:	Water Supply Potential of Seepage Ponds in the Coastal Area of Georgia
Project Number:	E-20-F08
Start Date:	7/1/1999
End Date:	6/30/2001
Research Category:	Engineering
Focus Category:	Water Supply, Surface Water, Hydrology
Descriptors:	Surface-agquifer linkages, Irrigation supply, Hydrologic budget
Lead Institute:	USGS
Principal Investigators:	Aris Peter Georgakakos, John S. Clarke

Publication

1. Peck, M.F., J.S. Clarke, M. Abu-Ruman, M.T. Laitta. 2001. "Hydrogeologic Conditions at Two Seepage Ponds in the Coastal Area of Georgia, August 1999 to February 2001." Proceedings of the 2001 Georgia Water Resources Conference, held March 26-27, 2001. The University of Georgia, Athens, Georgia.

The graduate student associated with USGS under this internship works on the project "Water Supply Potential of Seepage Ponds in the Coastal Area of Georgia".

Project Description: In the coastal area of Georgia, ponds are sometimes excavated at golf courses, farms, or communities by digging through sandy surface soils until the water table is reached. These man-made seepage ponds are often used to supply water for irrigation, and are thus a potential supplemental source of water to the Upper Floridan aquifer. Because the potential availability of water from seepage ponds is poorly understood in coastal regions, a test site will be selected for detailed evaluation.

Study objectives are to: (1) evaluate ground-water and surface-water relations at the pond; (2) develop a hydrologic budget for the pond-aquifer system; (3) determine the water-supply potential of the seepage pond; and (4) estimate vertical and horizontal hydraulic conductivity of the surficial aquifer in the vicinity of the pond. Results of the study will help define the potential availability of water from such ponds in similar settings. The proposed study involves site characterization and instrumentation, aquifer tests, and digital simulation of ground-water and surface-water relations in the vicinity of the pond. Data collection includes construction of test wells and minipiezometers, installation of ground-water level, pond-stage, and climatic recorders, and installation of seepage meters. Long-term aquifer tests are conducted to evaluate the water-supply potential of excavated ponds and to determine impacts on ground-water levels. Digital simulation of unstressed and aquifer-test conditions are used to evaluate pond an aquifer relations and to determine hydraulic properties of the surficial aquifer.

Intern Task Description: (1)Assist as an author in analysis, preparation, and publication of an interpretive scientific report of the pond-aquifer system at a test site in coastal Georgia. Prepare abstracts for presentation at technical conferences and make briefings at technical advisory committee meetings or other meetings as required. (2) Assist with more experienced hydrologists and hydrologic technicians in the collection and analysis of geologic, hydrologic, and climatic data from the pond test site. Site characterization includes development of a hydrogeologic framework and conceptual model of the flow system, evaluation of pond- and ground-water-level fluctuations, constructions of water-table maps, and development of a water budget for the pond-aquifer system. (3) Under guidance of experienced hydrologists, construct a digital ground-water flow model to simulate interactions between the pond and surficial aquifer system. These digital simulations, together with a long-term aquifer test will be used to provide an estimate of the water-supply potential of the aquifer.

This two-year internship is now approaching the end of its second year. The preliminary results of the study have been presented on a poster at the recent

Geological Society of America Conference, March 2000, and at the 2001 Georgia Water Resources Conference, March 2001.

Basic Information

Title:	Decision Support System for the Alabama-Coosa-Talapoosa (ACT) River Basin
Project Number:	E-20-F71
Start Date:	4/15/2000
End Date:	2/14/2002
Research Category:	Climate and Hydrologic Processes
Focus Category:	Hydrology, Management and Planning, Water Quantity
Descriptors:	Decision Support System, Reservoir Control and Operation, Water Resources Management and Planning, Ecological Integrity, Flood and Drought Management, Hydropower
Lead Institute:	Georgia Water Resources Institute
Principal Investigators:	Aris Peter Georgakakos

Publication

Problem and Research Objectives

The Alabama-Coosa-Tallapoosa (ACT) River Basin is shared by the states of Alabama and Georgia. The basin serves several water uses including agriculture, municipal and industrial water supply, hydropower, flood control, water quality, ecosystem protection, and recreation. The states of Alabama and Georgia have spent about six years negotiating a water allocation agreement. Many observers attribute the slow pace of the negotiation process to the absence of a shared set of comprehensive decision support tools capable of assessing the impact of the various water allocation proposals on the system. The objective of the Alabama-Coosa-Tallapoosa Decision Support System (ACT-DSS) project is to develop an advanced simulation-optimization decision support system for the ACT basin that can be used to assess the potential of the basin and investigate the impacts of alternative water allocation and management scenarios. GWRI has made the ACT-DSS available to the ACT stakeholders and has assisted them in using the system effectively during the negotiation process. Beyond the water allocation negotiation phase the model can be used to support water management.

Methodology

The Alabama-Coosa-Tallapoosa (ACT) Decision Support System consists of three main components: (1) a streamflow forecasting module, (2) a reservoir control component, and a (3) policy assessment module. The purpose of the streamflow forecasting component is to predict upcoming reservoir inflow and provide an appreciation of the forecast uncertainty through multiple forecast traces. The ACT-DSS inflow forecast model will generate forecast traces at all system nodes based on the statistical similarities of past inflows and those of the historical record. The second component of ACT-DSS is dedicated to reservoir control. Due to the need to satisfy multiple water uses over different time scales, this component includes three modules: (1) a turbine commitment and load dispatching module applicable to each hourly time step, (2) a short range control model operating on hourly time steps over a period of one week, and (3) a mid/long range control model operating on weekly time steps over a period of several months. This model configuration aims at generating system wide reservoir release policies subject to a set of specified constraints. The optimization operations are carried out by the Extended Linear Quadratic Gaussian (ELQG) control method. The three modules of the reservoir control component constitute a multi-level control hierarchy with an operational flow that follows two directions: the lower modules are activates first and generate information regarding performance functions and bounds. The mid/long range module uses these functions to develop system-wide reservoir management policies that satisfy the stated constraints and objectives. Once the long term policies have been identified, the lower level models can be activated again to determine the best turbine operation and loads implementing these decisions consistently across all relevant time scales. The last element of the ACT-DSS is the policy assessment component. Its purpose is to replicate the actual weekly operations of the ACT

system under various water allocations policies and operational scenarios. Namely, at the beginning of each week of the simulation horizon, this component invokes the inflow forecasting and reservoir control components, determines the most appropriate reservoir releases, simulates the response of the system for the upcoming week, and repeats this process at the beginning of the following decision time. At the completion of the forecast-control-simulation process, the program generates sequences of all system performance measures. These sequences can be used to compare the benefits and consequences of alternative water allocation and operation policies.

Principal Findings and Significance

At the request of the U.S. Environmental Protection Agency, GWRI has conducted scenario assessment of the water allocation agreement determined by the states of Alabama and Georgia. The results of this analysis have been presented to the Federal Commissioner and Federal Agencies responsible for reviewing the inter-state agreement to insure that it complies with applicable federal law. These parties have found the assessment results to be very useful in their review. Moreoever, U.S. Representative Bob Barr (of the 7th Congressional District of Georgia) and several other state and local government entities have requested the assessment results. Significant press coverage has been granted to the study in newspapers throughout Georgia and Alabama as well as the Associated Press and an Atlanta television station. The eventual impacts of the project are still to be determined as the negotiation process is still underway.

Basic Information

Title:	Ecological Impacts of Water Management Decisions for the Apalachicola-Chattahoochee-Flint River Basin in a Changing Climate
Project Number:	B-02-629-01
Start Date:	3/1/2000
End Date:	2/28/2001
Research Category:	Biological Sciences
Focus Category:	Nutrients, Surface Water, Water Quality
Descriptors:	Ecological integrity, Flow regime, Nutrient uptake, Organic matter production and loss
Lead Institute:	Georgia Water Resources Institute
Principal Investigators:	Judith Meyer

Publication

1. Gibson, C.A., and J.L. Meyer. 2001. "Ecosystem Services in a Regulated River: Variability in Nutrient Uptake and Net Ecosystem Metabolism in the Chattahoochee River." Proceedings of the 2001 Georgia Water Resources Conference, held March 26-27, 2001. University of Georgia, Athens, Georgia.

FINAL REPORT

Ecological Impacts of Water Management Decisions for the Apalachicola-Chattahoochee-Flint River Basin in a Changing Climate

Cathy Gibson and Judy Meyer
Institute of Ecology
University of Georgia
Athens, GA

Funded by: Georgia Water Resources Institute
Georgia Institute of Technology
Atlanta, GA

June 22, 2001

Problem and Research Objectives

The quantity and timing of river flow is critical to the ecological integrity of river systems (Poff et al. 1997). Flow is strongly correlated with physical and chemical characteristics of the river such as channel shape, water temperature and velocity, and habitat type and complexity (Jowett and Duncan 1990, Poff et al. 1997). In rivers that are regulated by dams, the flow regime is usually significantly altered when compared to the unregulated condition. Moreover, in a regulated situation baseflow conditions are almost completely determined by the dam operations. Thus, increases in water demand and/or decreases in water availability coupled with the concomitant changes in dam operation could dramatically alter the low flow conditions of an urban, regulated river such as the Chattahoochee River below Atlanta.

While there have been numerous studies examining the impact of changes in flow regime on specific species, there is little information about the potential relationship between flow regime and ecosystem functioning. In urban rivers, ecosystem processes such as nutrient uptake and processing of organic matter are essential to in-stream water quality both within the city and downstream. In rivers, nutrient uptake is often measured in terms of nutrient uptake length. Uptake length is defined as the average distance traveled by a molecule in the dissolved phase before it is incorporated into a particulate form or used by a consumer (Newbold et al 1983). Uptake length is strongly correlated with stream velocity (Newbold et al. 1983, Meyer and Edwards 1990, Webster and Ehrman 1996). Thus, changes in flow may influence the ability of the river biota to take up nutrients. Another ecosystem process that is essential to the maintenance of water quality is the processing of organic matter. Organic matter processing is most clearly measured through net ecosystem metabolism. Net ecosystem metabolism is simply gross primary production minus community respiration. There is little information about the relationship between flow and ecosystem metabolism. However, primary production has been shown to decrease after high flow events that scour away the primary producers (Uehlinger and Naegeli 1998).

We proposed to determine the extent of the current alteration of the flow regime due to dams, and to attempt to predict the magnitude of future flow regime alterations

under a future climate scenario and predicted management. Specifically we wanted to compare a pre-dam flow period (1938-1950) to a current climate and management period (1965-1995) to determine the impact of dams. Then we wanted to compare three different climate and management scenarios to separate the potential impacts of increasing demand from predicted future climatic scenarios: 1) current climate and management (1965-1995), 2) current climate (1965-1995) with 2050 management, and 3) predicted future climate (2018-2048) and 2050 management. This should help us determine the type and magnitude of flow alterations that are possible for the river in the future. We can then determine what the impacts of these flow alterations might be on ecosystem functioning.

We also proposed to evaluate the relationship between flow and two critical ecosystem functions, nutrient uptake length and net daily metabolism, in order to predict how changes in flow regime affect ecosystem function. Our objective was to determine how nutrient uptake lengths and net ecosystem metabolism varied under different baseflow conditions in the Chattahoochee River below Atlanta. This research should give us a more holistic view of the river and a better understanding of how management affects the functioning of the river.

Methodology

We quantified the changes in flow regime through the use of the Indicators of Hydrologic Alteration (IHA) program (Richter et al. 1996). This program takes daily stream flow values and calculates indices relating to the five components of flow regime critical for ecological processes: magnitude, frequency, duration, timing, and rate of change of hydrologic conditions. Specifically, IHA determines mean monthly flow and the inter-annual variability of the mean flow for each month. IHA determines the magnitude of the 7, 30, and 90-day minima and maxima and the inter-annual variability of each of these flows. In terms of frequency, IHA calculates the mean number and duration of low and high pulses in the system. In terms of timing, the program also calculates the day on which the minimum and maximum occur and the inter-annual variability of these events.

We examined the relationship between flow and ecosystem function through measures of nutrient uptake length and net daily metabolism on the Chattahoochee River below Atlanta, Georgia. We used the USGS real time gauging station at Fairburn, GA (station # 02337170) and at State Road 280 near Atlanta (station # 02336490) to obtain discharge every 15 minutes.

Nutrient uptake length was measured using the methods described by Webster and Ehrman (1996) and Stream Solute Workshop (1990). We used effluent of wastewater treatment plants as the source of the conservative tracer (chloride, Cl^-) and soluble reactive phosphorus (SRP) (Marti et al. in press). We sampled SRP, and Cl^- concentration at one site above and five sites below the major municipal discharges from Atlanta on four different days during summer 2000. The most upstream site was the Highway 166 crossing; the next four sites were 5.2, 21.8, 39.1, and 46.6 km downstream respectively. The site above Atlanta was used to correct for background concentrations. All samples were taken during baseflow, filtered in the field with Gelman A/E glass fiber filters, and stored on ice for transport to the lab. Samples were then frozen until nutrient analysis could be performed. SRP concentration was determined using the colormetric methods of Wetzel and Likens (1992). Chloride was determined with an ion chromatograph (UGA Soil Ecology Lab). SRP uptake length is the inverse of the slope of the regression line between distance (km) and ln (SRP : chloride ratio) after correcting for background concentrations (Webster and Ehrman 1996). In cases where the SRP: chloride ratio increased downstream we assumed that there was no uptake, since this implies a net release of SRP from the sediments.

We determined net daily metabolism for a 1.4 km reach just above Highway 166 using the upstream-downstream diurnal dissolved oxygen change technique (Marzolf et al. 1990, Young and Huryn 1998). We determined travel time for a variety of discharges by floating oranges from the upstream to downstream station. Travel time was estimated from the median orange. We continuously measured dissolved oxygen and temperature using a Hydrolab dissolved oxygen probe for a 40-hour period. Oxygen concentrations were corrected for diffusion using the energy dissipation model (APHA 1992). Channel slope for this model was determined by using 1:24,000 USGS topographic maps and determining the average slope for the river between Atlanta and West Point Lake.

Principal Findings and Significance

Implications of Climate Change on Flow Regime for Chattahoochee River at Whitesburg

Though the pre-dam record is relatively short, flow before the construction of dams was typified by high winter and spring flows and lower summer and especially fall flows (Figure 1a.). The construction of dams along the Chattahoochee River north of Whitesburg resulted in an approximately 1000 cfs increase in summer flows (Figure 1a). However, expected increases in demand for water to levels expected in 2050 will decrease summer and fall flows (June – October) even without any climate change (Figure 1b). Management changes and expected demand increases will lead to decreased mean monthly flow in the summer and fall by almost 1000 cfs. Under predicted future climate scenarios and 2050 demand, summer flows will decrease even further (Figure 1b.). Mean monthly flow for summer months (June-September) are predicted to decrease another 500 to 1000 cfs. Under current climate and demand, mean flow in the Chattahoochee River at Whitesburg, Ga for the summer months of June through September is 3500 cfs. Under 2050 demand and future climate scenarios, average flow for these months is predicted to be 2000 cfs.

The average 7, 30, and 90 day maximum flows are similar among the three water conditions (pre-dam construction, current conditions, and current climatic conditions but increased demand) (Figure 2). However, under future climate scenarios and expected demand, the 7, 30, and 90 day maxima are all lower than current conditions and current conditions with 2050 demand (Figure 2).

The average 7, 30, and 90 day minima increased after construction of the dams (Figure 3). Demand increases expected in the future lower the 30 and 90 day minima, but have little impact on the 7 day minimum (Figure 3). Future climate scenarios combined with expected demand increases are predicted to lower the minimum flow over all three time scales, 7, 30, and 90 days (Figure 3). However, these low flows are still higher than those experienced from 1938-1950.

Construction of dams decreased the variability of flow in the river during summer and winter and slightly increased flow variability in the spring (Figure 4). Increases in demand under current climate conditions would slightly increase the variability of the system in the summer. Future climate scenarios coupled with future demand would decrease variability of river flow throughout the year (Figure 4).

Variability of Nutrient Uptake and Net Ecosystem Metabolism under Different Baseflow Conditions

The Chattahoochee River at Highway 166 is a highly heterotrophic system. SRP uptake length for this 46 km reach of the river ranged from no uptake at all to 232 km (Table 1). Highly negative net ecosystem metabolism, low P/R ratios, and high rates of respiration demonstrate that this system is fueled by allochthonous carbon and that a large amount of organic matter processing is occurring. In contrast, long uptake lengths and evidence of a lack of uptake suggests that there is little assimilation of the nutrients from the wastewater treatment plants.

There was no clear relationship between SRP uptake length and discharge (Table 1). There was also no clear relationship between discharge and net ecosystem metabolism (Figure 5). However, it did appear that gross primary production, one of the two components of net ecosystem metabolism, increased with increasing discharge (Figure 6). The Chattahoochee River below Atlanta is a sandy bottom river, with little stable substrate. The predominant stable substrate in this section of the river is the large snags along the banks. As discharge increase, more snag area is inundated, and therefore there is more substrate available to the primary producers like diatoms. We will be examining this relationship between available snag habitat and gross primary production more thoroughly in future research.

SRP uptake lengths (104 and 232 km) in this study were almost two orders of magnitude longer than those found in a river with similar discharge, but not receiving any waste water treatment plant effluent (1.5 km) (Butturini and Sabater 1998). Third order Mediterranean streams receiving wastewater treatment plant effluent also had much longer SRP uptake lengths than non-polluted streams with similar discharge (Marti et al

in press). Similar to our study, phosphorus concentrations in the Mediterranean streams receiving effluent did not consistently decline downstream in 33% of the cases (Marti et al. in press). In our study, the instances of no measurable uptake were associated with an increase in phosphorus concentrations in the downstream direction and a concomitant positive relationship between phosphorus : chloride ratio and distance downstream. This increase in phosphorus concentrations could be caused by the flux of phosphorus out of the sediments (Reddy et al. 1996).

The long uptake lengths as well as the increase in phosphorus concentrations downstream in this reach of the river have major implications for water quality in West Point Lake. The distance between the Highway 166 crossing and Franklin, GA (the site of the river/reservoir transition) is 76 km. The shortest uptake length measured in this study was 104 km. Therefore, the average phosphorus molecule will have not been assimilated prior to reaching West Point Lake. This means that a majority of the phosphorus from Atlanta's municipal wastewater facilities is directly discharged into West Point Lake. This high phosphorus loading could lead to eutrophication of the reservoir and algal blooms. In addition, these long uptake lengths indicated that the river may no longer be capable of retaining and transforming phosphorus during some times of the year. Therefore, the river is no longer capable of providing the service of nutrient assimilation to downstream water users.

In contrast, organic matter processing rates seem fairly high. P/R ratios ranged from 0.2 to 0.4 indicating that this is a heterotrophic system, which is dominated by allochthonous inputs. These P/R ratios are well within the range of P/R ratios (0.02 to 0.4) found in the Ogeechee River, which is dominated by allochthonous organic matter inputs from the floodplain (Meyer and Edwards 1990).

These findings are described in greater detail in the attached publication (Gibson and Meyer 2001). Measurements of nutrient uptake and ecosystem metabolism are continuing. Measures of ecosystem processes under a wider range of discharges will enaable us to better determine the nature of the relationship between in stream flow and ecosystem function.

Literature Cited

APHA, AWWA, and WEF. 1992. Standard Methods for the Examination of Water and Wastewater. 18th ed. American Public Health Association, Washington DC.

Butturini and F. Sabateur 1998 Ammonium and phosphate retention in a Mediterranean stream: hydrological versus temperature control. Canadian Journal of Fisheries and Aquatic Sciences 55: 1938-1945.

Gibson, C.A. and J.L. Meyer. 2001. Ecosystem services in a regulated river: variability in nutrient uptake and net ecosystem metabolism in the Chattahooche River. in K. Hatcher (ed.) Proceedings of the 2001 Georgia Water Resources Conference.

Jowett, I.G. and M.J. Duncan. 1990. Flow variability in New Zealand rivers and its relationship to in-stream habitat and biota. New Zealand Journal of Marine and Freshwater Research 24: 305-317.

Marti, E., J. Aumatell, L. Gode, M. Poch, and F. Sabateur. In press. Effects of wastewater treatment plant inputs on stream nutrient retention. Water Resources Research.

Marzolf, E.R., P.J. Mullholland, and A.D. Steinman.1994. Improvements to the diurnal upstream-downstream dissolved oxygen change technique for determining whole-stream metabolism in small streams. Canadian Journal of Fisheries and Aquatic Sciences 51: 1591-1599.

Meyer, J.L. and R.T. Edwards. 1990. Ecosystem metabolism and turnover of organic carbon along a blackwater river continuum. Ecology 71: 668-677.

Newbold, J.D., J.W. Elwood, R.V. O'Neill, and A.L. Sheldon. 1983. Phosphorus dynamics in a woodland stream ecosystem: a study of nutrient spiralling. Ecology 64: 1249-1265.

Poff, N.L., J.D. Allan, M.B. Bain, J.R. Karr, K.L. Prestegaard, B.D. Richter, R.E. Sparks, J.C. Stromberg. 1997. The natural flow regime; a paradigm for river conservation and restoration. BioScience 47: 769-784.

Richter, B.D., J.V. Baumgartner, J. Powell, and D.P. Braun. 1996. A method for assessing hydrologic alteration within ecosystems. Conservation Biology 10: 1163-1174.

Stream Solute Workshop. 1990. Concepts and methods for assessing solute dynamics in stream ecosystems. Journal of the North American Benthological Society 9: 95-119.

Uehlinger, U. and M.W. Naegeli. 1998. Ecosystem metabolism, disturbance, and stability in a prealpine gravel bed river. Journal of the North American Benthological Society 17: 165-178.

Young, R.G. and A.D. Huryn. 1998. Comment: Improvements to the diurnal upstream-downstream dissolved oxygen change technique for determining whole-stream metabolism in small streams. Canadian Journal of Fisheries and Aquatic Sciences 55: 1784-1785.

Webster, J.R. and T.P. Ehrman. 1996. Solute dynamics. In *Methods in Stream Ecology* F.R. Hauer and G.A. Lamberti (editors). Academic Press, San Diego, CA. pp. 145-160.

Wetzel, R.G. and G.E. Likens. 1992. Limnological Analyses. Springer-Verlag, New York, NY.

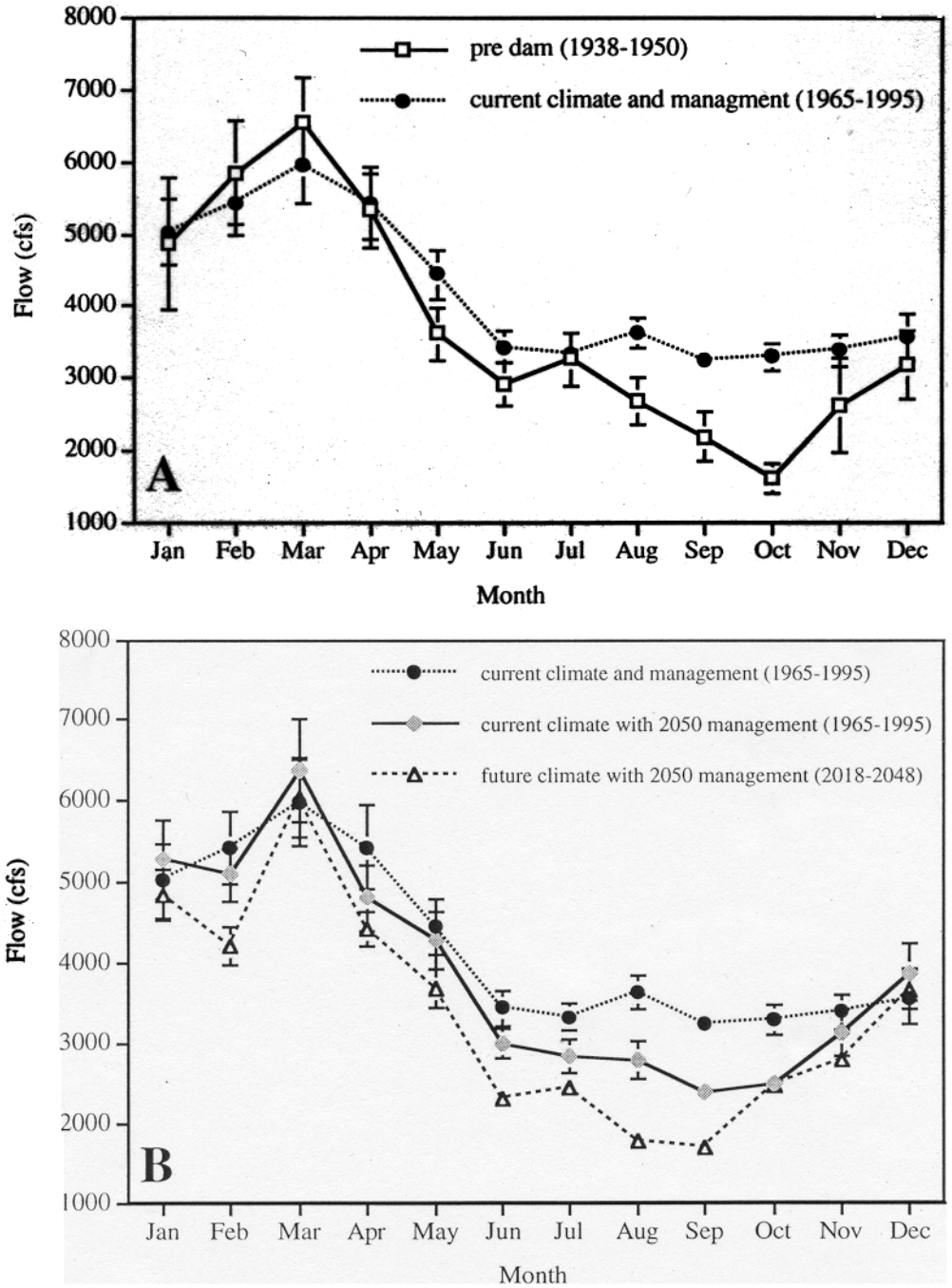

Figure 1: Mean monthly flow of the Chattahoochee river at Whitesburg, GA under different management and climate scenarios: A) pre-dam conditions and current climate and management (1965-1995). B) current climate and management (1965-1995); current climate (1965-1995) and 2050 management ; predictued future climate (2018-2048) and 2050 water demand. Error bars are ± standard error. Flow scenarios provided by A. Georgakakos, Georgia Insitute of Technology.

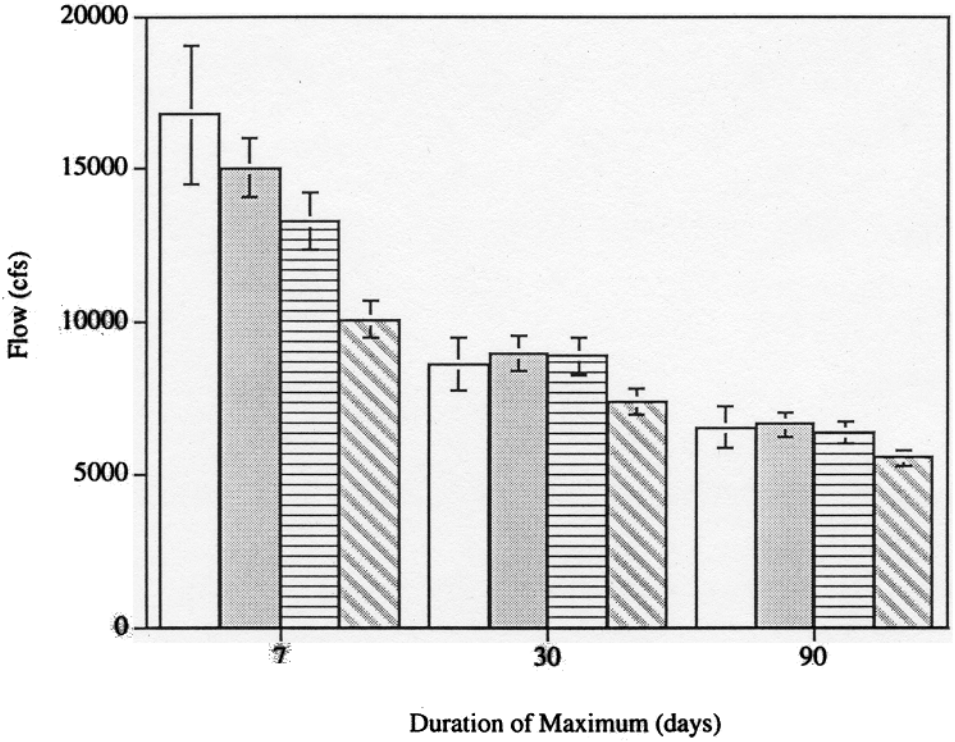

Figure 2: 7, 30, and 90 day maximum flows of the Chattahoochee River at Whitesburg, GA under four different climate and management scenarios: 1) pre-dam conditions (1938-1950), 2) current climate and management (1965-1995), 3) current climate (1965-1995) and 2050 management, 4) predicted future climate (2018-2048) and 2050 management. Error bars are ± standard error. Flow scenarios provided by A. Georgakakos, Georgia Institute of Technology.

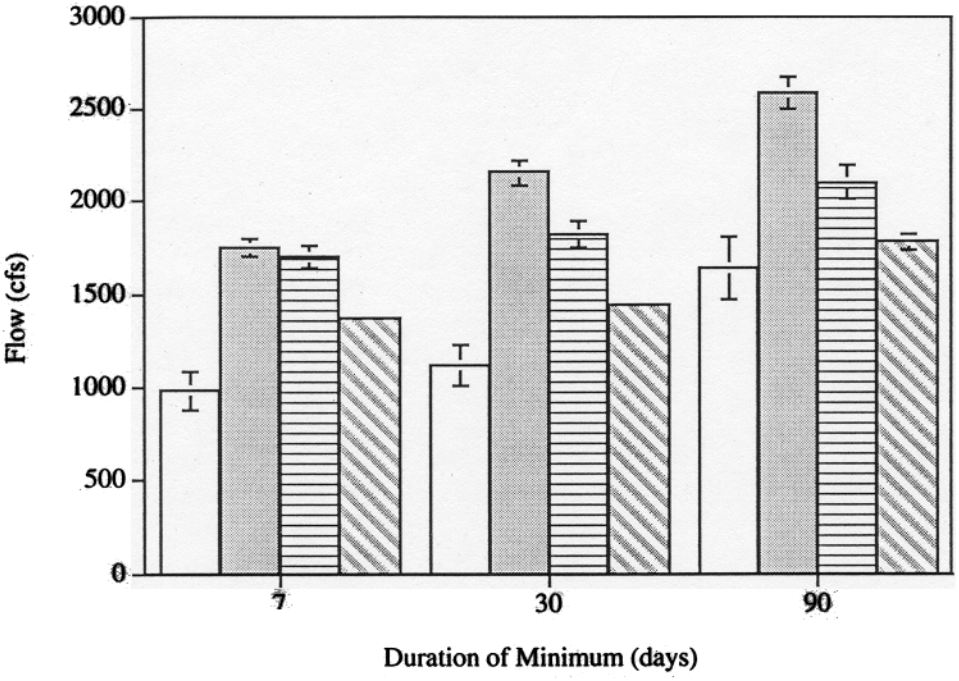

pre dam (1938-1950)

current climate (1965-1995) and management

current climate (1965-1995) and 2050 management

future climate (2018-2048) and 2050 managment

Figure 3: 7, 30, and 90 day minimum flows of the Chattahoochee River at Whitesburg, GA under four different climate and management scenarios: 1) pre-dam conditions (1938-1950), 2) current climate and management (1965-1995), 3) current climate (1965-1995) and 2050 management, 4) predicted future climate (2018-2048) and 2050 management. Error bars are ± standard error. Flow scenarios provided by A. Georgakakos, Georgia Institute of Technology.

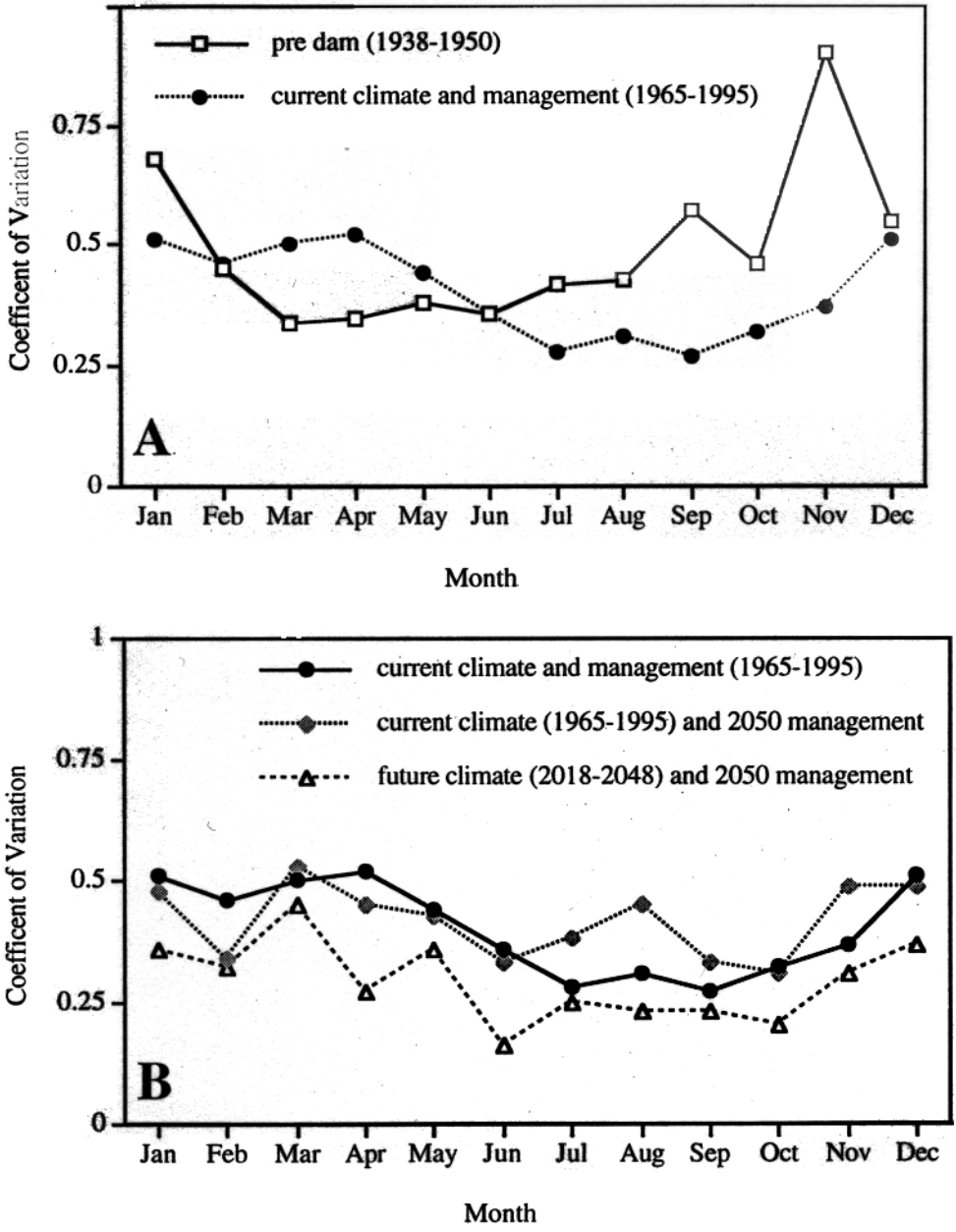

Figure 4. Coefficent of variation for mean monthly flow of the Chattahoochee River at Whitesburg, GA. A) Comparison of variation of two different climate and management scenarios pre-dam conditions (1938-1950) and current climate and management (1965-1995). B) Comparison of three different climate and managment secenarios: current climate and management (1965-1995); current climate (1965-1995) and future management (2050); and predicted future climate (2018-2048) and management (2050). Flow scenarios provided by A. Georgakakos, Georgia Institute of Technology.

Table 1: SRP uptake length for the 46 km reach below the Highway 166 crossing. Net ecosystem metabolism for a 1.4 km reach upstream of the Highway 166 crossing.

Date	Discharge (m^3/s)	Temperature (°C)	Initial SRP concentration (µg/l)	SRP uptake (km)	Gross Primary Production ($g\ O_2\ m^{-2}\ d^{-1}$)	Respiration ($mg\ O_2\ m^{-2}\ d^{-1}$)	Net Ecosystem Metabolism ($g\ O_2\ m^{-2}\ d^{-1}$)
June 26	46	24.6	62	104	2.08	7.22	-5.14
July 3	28	26.1	41	No uptake	0.64	3.04	-2.40
July 17	32	28.5	113	232	1.37	6.61	-5.24
August 7	37	26.3	66	No uptake	1.45	5.59	-4.14

Basic Information

Title:	Ribotype Source Library of Escherichia Coli Isolates from Georgia
Project Number:	B-02-629-G1
Start Date:	3/1/2000
End Date:	2/28/2001
Research Category:	Biological Sciences
Focus Category:	Water Quality, Surface Water, Non Point Pollution
Descriptors:	Coliform isolation, Pollution source assessment, Pollution transport assessment, Pollutant source control
Lead Institute:	Georgia Water Resources Institute
Principal Investigators:	Peter Hartel

Publication

FINAL REPORT TO THE GEORGIA WATER RESOURCES INSTITUTE

Ribotype Source Library of *Escherichia coli* Isolates from Georgia

March 1, 2000 to February 28, 2001

Peter G. Hartel
Dept. of Crop & Soil Sciences
University of Georgia
Athens, GA 30602-7272

Problem and research objective

Fecal coliforms consist of several bacterial genera from the family Enterobacteriaceae that can grow on a selective medium at 44.5˚C for 24 hours. Fecal coliforms normally inhabit the intestinal tract of warm-blooded animals and their presence in soil or water is a good indicator that the soil or water was contaminated by bacterial pathogens. For example, when numbers of fecal coliforms exceed 2,000 per 100 mL of water, the likelihood of bacterial pathogens in the water is 98.1% (Geldreich, 1970). Fecal coliform counts are typically used to monitor Georgia's recreational waters.

One of the most vexing problems in isolating fecal coliforms from water samples is not knowing the host origin of these bacteria. In the past, the only way to identify the host origin of a bacterium was to observe the bacterium's various phenotypic markers (i.e., characteristics expressed by the bacterium, like antibiotic resistance). The main problems with using phenotypic markers are their lack of reproducibility and lack of discriminatory power (ability to distinguish two closely related strains). However, in recent years, it has become possible to identify the host origin of a bacterium based on its DNA. This alternative method, called genotyping, not only has increased reproducibility, but also has increased discriminatory power. The most common of these genotypic methods include chromosomal DNA restriction analysis, plasmid typing, pulsed field gel electrophoresis, various polymerase chain reaction (PCR) methods, and ribotyping (Farber, 1996).

Each genotypic method has its advantages and disadvantages with respect to strains that can be typed, reproducibility, discriminatory power, ease of interpretation, and ease of performance. In this report, the genotypic method selected was ribotyping. Ribotyping is based on ribosomal RNA (rRNA). Ribosomal RNA is present in all bacteria, and is composed of three species, 5S, 16S, and 23S. The DNA in the bacterium that encodes for these three species of rRNA is usually present in 2 to 11 copies and is highly conserved (does not mutate; Grimont and Grimont, 1986). In ribotyping, the DNA is isolated from the bacterium and cut with a special enzyme that only recognizes certain DNA sequences (i.e., a restriction enzyme). The DNA is electrophoresed in a gel and the DNA transferred to a nylon membrane (this is called Southern blotting). The membrane is probed with a chemiluminescent copy of the 5S, 16S, and 23S portions of the DNA and, when properly treated, the membrane gives a pattern that can be scanned with an imager. As a method for distinguishing a subspecies of a bacterium, ribotyping is considered to have excellent reproducibility, good discriminatory power, excellent ease of interpretation, and good ease of performance (Farber, 1996).

Here, the fecal coliform selected for ribotyping was *Escherichia coli*. This bacterium was selected for five reasons. First, as a fecal coliform, *E. coli* is accepted by the American Public Health Association as a good indicator of pathogenic bacteria (Clesceri et al., 1998). Second, most environmental ribotyping has been done with this bacterium. As a result, the methodology for ribotyping this bacterium is established. Third, there is good scientific evidence that specific strains of *E. coli* are associated with different host species (e.g., Amor et al., 2000). Fourth, *E. coli* does not exist as a stable population in the environment unless the source of contamination is persistent. Fifth, *E. coli* is easy to isolate and easy to manipulate genetically.

With an extensive library of *E. coli* ribotypes from Georgia, one should be able to isolate *E. coli* from any water source (as well as from other sources, like soil) in Georgia and identify the host origin of that *E. coli* isolate. To develop this library, a large number of *E. coli* isolates must be obtained from warm-blooded animals and ribotyped. An isolate of *E. coli* from a water source can then be ribotyped and compared to the source library to identify its host.

Therefore, the objective of the research was to construct a ribotype source library of *E. coli* isolates from a wide variety of warm-blooded animals in Georgia in order to determine the host origin of *E. coli* isolates from Georgia waters. However, in addition to obtaining *E. coli* isolates from Georgia, isolates were also obtained from a) Idaho in order to assess the biogeographic variability of the *E. coli* ribotypes, and b) the Chattahoochee River under conditions of wet weather and base flow conditions in order to assess the biodiversity of *E. coli* ribotypes under these conditions.

Methodology

Selection and identification of E. coli isolates from various host sources in Idaho and Georgia

Isolates of *E. coli* were obtained directly from the animal feces of cattle, horse, and swine in the vicinity of Kimberly, Idaho, and Athens, Brunswick, and Tifton, Georgia (Fig. 1).

Fig. 1. Location and distance among the four sampling sites in Georgia and Idaho. At each location, isolates of *E. coli* were obtained from cattle, horse, and swine.

Because Georgia is ranked first in the United States for broiler production (Georgia Agricultural Statistics Service, 1999), *E. coli* isolates were also obtained from poultry in the three Georgia locations. Whenever possible, at least 25 isolates from each species at each location was obtained. Fresh feces were sampled with a culture swab containing Cary–Blair medium (Becton Dickinson, Sparks, MD). Swabs were kept on ice for a maximum of 24 h before streaking the swab on 5-cm petri dishes containing mTEC medium (Difco Laboratories, Sparks, MD). Plates were incubated submerged in a water bath at 44.5±0.2°C for 24 h according to Standard Methods (Clesceri et al., 1998). Yellow isolates were randomly selected, streaked onto tryptic soy agar (Difco), and incubated at 35°C for 24 h. The streaking was repeated twice to ensure the purity of each isolate. Each isolate was inoculated into a multiwell tissue culture plate containing separate 1-mL slants of Simmons citrate and urea agar (both Difco). Three bacterial species obtained from the American Type Culture Collection (ATCC; Manassas, VA), *Escherichia coli* ATCC #11775 (citrate negative, urea hydrolysis negative),

Klebsiella pneumoniae ATCC #13883 (citrate positive, urea hydrolysis positive), and *Enterobacter aerogenes* ATCC #13048 (citrate positive, urea hydrolysis negative), were the controls. Isolates that were both citrate- and urea hydrolysis-negative were subjected to an oxidase test (MacFaddin, 1976). Isolates that were oxidase negative were considered *E. coli* and kept for long-term storage. To do this, a loopful of each isolate (approximately 40 mg) was removed from the tryptic soy agar plate, placed in a mixture of saline–phosphate (NaCl, 8.5 g L^{-1}, K_2HPO_4, 0.65 g L^{-1}; KH_2PO_4, 0.35 g L^{-1}; pH 7.0; 700 µL), glycerol (100 µL) and dimethyl sulfoxide (100 µL), and stored at –70°C.

Selection and identification of E. coli isolates from the Chattahoochee River

The study area was a 77-km reach of the Upper Chattahoochee Watershed (Fig. 1). There were a total of twelve sampling sites, consisting of eight tributary sites and four Chattahoochee River sites. This reach of the Chattahoochee was selected because it is one of the most heavily used rivers in Georgia, serving as a resource for drinking water, recreation, and wastewater assimilation for much of metropolitan Atlanta. According to the Georgia Department of Natural Resources (1997), 67 of 77 stream reaches assessed in metropolitan Atlanta did not meet or only partially met water quality standards. Excessive numbers of fecal coliform bacteria were a contributing factors in 63 of these 67 streams. Generally, median numbers of fecal coliforms in the water increase steadily from <20 Most-Probable-Number (MPN) per 100 mL below Buford Dam to 790 MPN per 100 mL downstream of metropolitan Atlanta (Gregory and Frick, 2000).

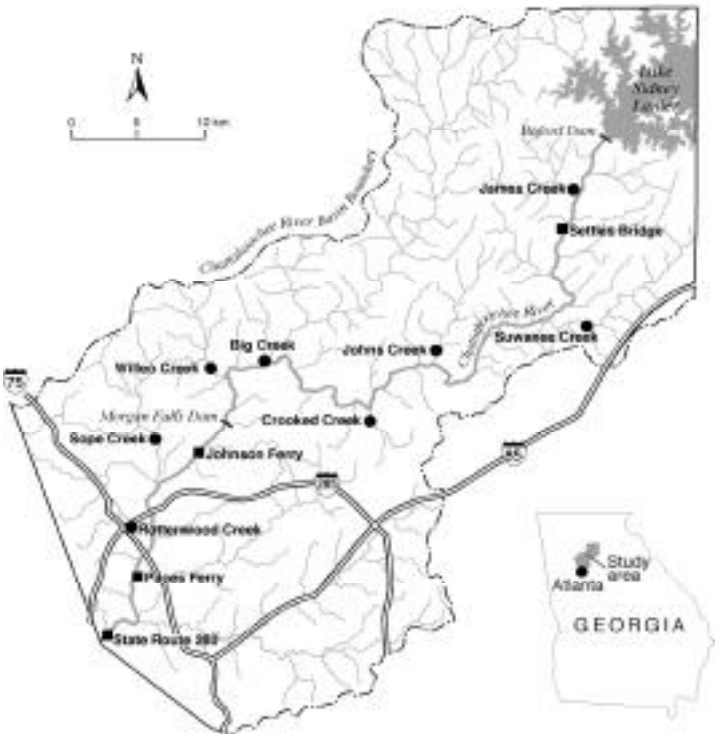

Fig. 2. Location of the sampling sites, comprising eight tributary streams (closed circles) and four main stem sites (closed squares) of the Upper Chattahoochee River Watershed, Georgia. The tributaries and main stem sites encompass the Chattahoochee River National Recreation Area. The northwest and southeast boundaries represent the limits of the Chattahoochee River Basin.

Water sampling

Water samples for base flow and wet weather conditions were collected on 22 Feb 2000 and 2 Apr 2000, respectively. With the exception of James Creek during wet weather conditions, all samples were collected with isokinetic, depth-integrated samplers (Models D-77, DH-59, DH-81, or DH-95, U.S. Geological Survey Hydrological Instrumentation Facility, Stennis Space Center, MS). All samples from the mainstem of the Chattahoochee River during base flow and wet weather conditions were sampled from a bridge or boat. With the exception of James Creek during wet weather conditions, all samples from the tributaries were sampled by wading during base flow conditions and from bridges during wet weather conditions. During wet weather conditions, James Creek was sampled with a grab sample because flow conditions made it unsafe for wading.

Surface water samples were collected according to U.S. Geological Survey protocols (Myers and Wilde, 1999; Wilde et al., 1999). Briefly, approximately 1 to 3 L of water was collected at each site on each sampling date. At each sampling site, the width of the river or tributary was measured and divided into at least five equal increments. At each of these points, one sample was collected continuously from the surface to a point near the bottom. All the samples at one site were composited. In this manner, one depth-integrated, equal-width-increment sample was obtained from each site, eliminating much of any horizontal and vertical sampling bias.

Samples were transported from streams to the laboratory on ice in coolers and were processed within 6 hours. Each 10- and 100-mL water sample was passed through separate 0.45-µm filters, each filter was placed on 5-cm petri dish containing mTEC medium as mentioned previously.

DNA extraction and quantification

Isolates of *E. coli* were streaked on tryptic soy agar and incubated at 35°C for 24 h. A single clone was inoculated into 10 mL of Luria-Bertani broth (pH 7.5; Sambrook et al., 1989) contained in a 16 by 150 mm test tube and placed on a rotating shaker at 75 rpm at 35°C. After 18 h, a 2.0-mL sample was removed and the DNA extracted with a commercial kit (Qiagen DNeasy, Qiagen, Valencia, CA). A portion of the DNA was mixed with Hoechst Dye #33258 (Amersham Pharmacia Biotech, Piscataway, NJ) according to the manufacturer's directions and was quantified with a fluorometer (DynaQuant DQ200, Amersham Pharmacia Biotech). DNA from *E. coli* strain B (Sigma Chemical Co., St. Louis, MO) was the standard.

Ribotyping of E. coli isolates

Separate 1-µg samples of *E. coli* DNA were digested overnight, one with the enzyme *Eco*RI and the other with *Pvu*II, both according to the manufacturer's specifications (Roche Molecular Biochemicals, Indianapolis, IN). The digested DNA was stained with bromphenol blue–xylene cyanole tracking dye (Sigma) and was electrophoresed in a 1.0% agarose gel at 58 volts for 3 hours. The gel was run submerged in TAE buffer (40 m*M* Tris-Acetate and 1 m*M* EDTA; FisherBiotech, Fair Lawn, NJ) in an horizontal gel rig (12 by 14 cm gel size, Easycast™ Model B2, Owl Separation Systems, Portsmouth, NH) with a power supply (Model EC105, E-C Apparatus Corp., Holbrook, NY). Digoxigenin-labeled (DIG-labeled) Molecular Weight Marker III (Roche), consisting of λ DNA cleaved with the restriction enzymes *Eco*RI and *Hind*III, occupied every fifth lane of the gel. Additional lanes were no DNA (control) and DNA from the *E. coli* ATCC #11775. The DNA in the gel was denatured with a solution containing 0.5 M NaOH and 1.5 M NaCl, and was neutralized with a buffer containing 0.5 M Tris–HCl and 1.5 M NaCl (pH 7.0). The DNA was transferred to a nylon membrane (Nytran supercharged membrane, Schleicher and Schuell, Keene, NH) with a vacuum blotting system (VacuGene™ XL, Pharmacia Biotech) as per the manufacturer's directions. The DNA on the membrane was crosslinked with 120 MJ cm^{-2} of UV light (Model XL-1000 Spectrolinker, Spectronics Corporation, Westbury, NY). The membrane was covered in prehybridization buffer containing formamide (50 ml per 100 mL of water) and placed in a hybridization oven (Model HB-1D, Techne Inc., Princeton, NJ) at 42 °C for 2 h. Following prehybridization, the

DNA was hybridized with a DIG-labeled probe at 42 °C overnight. To prepare the DIG-labeled probe, total *E. coli* ribosomal RNA (Sigma) was reverse transcribed with reverse transcriptase, hexanucleotide mix, and dNTP (all Roche) into cDNA according to the manufacturer's instructions. To inactivate all RNases during the DIG-labeling, all distilled water in the reaction was treated with diethylpyrocarbonate (1.0 mL L^{-1}; Sigma). The distilled water–diethyl pyrocarbonate mix was incubated overnight at 37°C before autoclaving at 121 °C for 2 h.

To prepare the membranes for chemiluminescence, membranes were washed twice for 5 min in 2X SSC (0.3 M NaCl and 0.03 M sodium citrate)–0.1% sodium dodecyl sulfate (1.0 mL L^{-1}; SDS) at 42°C, and twice for 15 min with 0.5X SSC–0.1% SDS at 55°C. Washed membranes were treated with washing buffer (pH 7.5) containing Tween 20 (3.0 mL L^{-1}), maleic acid (0.1 M), and NaCl (0.15 M) for 1 min at room temperature (20 to 22 °C), and incubated on an orbital shaker for 1 hour in 1X blocking buffer containing blocking reagent (Roche) and maleate buffer (0.1 M maleate and 0.15 M NaCl; pH 7.5). Membranes were incubated in the same buffer amended with 1:10,000 dilution of anti-DIG alkaline phosphatase Fab fragments (Roche). The membranes were treated twice with washing buffer for 15 min at room temperature and treated with 100 mM Tris Base–100 mM NaCl (pH 9.5) for 2 min. Membranes were placed between acetate page protectors and a chemiluminescent substrate for alkaline phosphatase was added (CSPD, Roche). Membranes were imaged (Model FluorChem™ 8000, Alpha Innotech, San Leandro, CA) and images saved as a TIFF file. TIFF files were imported into GelComparII (Applied Maths, Kortrijk, Belgium) for analysis. Typically, gels showed 9 to 11 bands for *Eco*RI and 9 to 11 bands for *Pvu*II; this was considered sufficient for good discrimination among ribotypes. DNA fragments <1375 base pairs were also discarded because they were often indistinct. Lanes were normalized within the gel with DIG-labeled Molecular Weight Marker III and variations among the gels were assessed with the *E. coli* ATCC #11775 strain. Optimization (shift allowed between any two patterns) and tolerance (maximum distance allowed between two band positions on different patterns) were each set at 1.00%. Similarity indices were determined using Dice's coincidence index (Dice, 1945) and the distance among clusters calculated using the unweighted pair-group method using arithmetic averages (UPGMA). Based on variability of the inter-gel *E. coli* control, banding patterns had to be greater than or equal to 90 percent similar to be considered the same ribotype.

Principal findings and significance

The objective of the project was to obtain the ribosomal DNA fingerprint (ribotype) of 1,000 isolates of *E. coli* from the feces of a wide variety of warm-blooded animals, including humans, from four locations in the State of Georgia. We have ribotyped 2,000 isolates of *E. coli* (Table 1; next page). Although the proposal stated that we would put the ribotype patterns on the web, we have refrained from doing so because of their high monetary value. The complete list of the ribotyped isolates is available from the author.

With regards to biogeographic variability, total of 568 *E. coli* isolates from Kimberly, Idaho (125 isolates), and Athens (210 isolates), Brunswick (102 isolates), and Tifton, Georgia (131 isolates) yielded 211 ribotypes for an isolate:ribotype ratio of 2.7:1. The percentage of ribotype sharing within an animal species increased with decreased distance for cattle and horses, but not for swine and poultry. The maximum percentage of ribotype sharing was 20%. When the *E. coli* ribotypes among the hosts were compared at one location, the percent of unshared ribotypes was 86, 89, 81, and 79% for Kimberly, Athens, Brunswick, and Tifton, respectively. These data suggest that there is good ribotype separation among host animal species at one location, and that the ability to obtain good host origin matching depends on a large number of isolates and a distance <175 km for certain host animal species.

Table 1. Host animal species and number of *E. coli* isolates ribotyped from each species. All isolates are from Athens, Atlanta, Brunswick, or Tifton, Georgia.

Species	Number of Isolates
Bear	11
Beaver	5
Cattle	879
Deer	230
Dog	52
Duck	3
Emu	3
Fox	4
Geese	54
Goat	74
Horse	106
Human	185
Ostrich	3
Poultry	156
Rabbit	2
Rhea	3
Seabirds	36
Sheep	68
Swine	126
Total	2000

With regards to ribotype diversity in the Chattahoochee River under wet weather and base flow conditions, a total of 630 *E. coli* isolates was obtained from water samples collected during synoptic surveys of eight tributaries and four main stem sites from February to April 2000. Synoptic surveys targeted base flow and wet weather conditions. During base flow conditions, there was a total of 162 ribotypes (239 isolates), of which 97 (125 isolates) were unique; during wet weather conditions, there was a total of 86 ribotypes (107 isolates), of which 57 (69 isolates) were unique. To be unique, a ribotype could only be observed in one location during base flow or wet weather conditions. The large number of unique ribotypes suggests that considerable ribotype heterogeneity exists, and that a large number of *E. coli* isolates is needed to obtain a representative sample of ribotypes from watersheds with complex land use patterns and varied flow conditions.

Publications resulting from the project

Journal articles (submitted or in preparation)

Hartel, P. G., J. D. Summer, J. L. Hill, J. V. Collins, J. A. Entry, and W. I. Segars. 2001. Biogeographic variability of *Escherichia coli* ribotypes from Idaho and Georgia. J. Environ. Qual. (submitted)

Hartel, P. G., A. L. Funk, J. D. Summer, J. L. Hill, E. A. Frick, and M. B. Gregory. 2001. Ribotype diversity of *Escherichia coli* isolates from the Upper Chattahoochee River Watershed in Georgia. J. Environ. Qual. (in preparation).

Abstracts (in print)

Funk, A. L., M. B. Gregory, E. A. Frick, and P. G. Hartel. 2000. Microbial source tracking using ribosomal RNA typing in the Chattahoochee River National Recreation Area Watershed, Metropolitan Atlanta, Georgia—Study design and preliminary results. Building capabilities for monitoring and assessment in public health microbiology, U. S. Geological Survey, March 14-16, Columbus, OH.

Godfrey, D. G., and P. G. Hartel. 2001. Geographic variability of *Escherichia coli* ribotypes from swine feces in Georgia and Idaho. National Conference on Undergraduate Research, March 15-17, Lexington, KY.

Hartel, P. G., J. D. Summer, W. I. Segars, and J. Entry. 2000. Geographic variability of *Escherichia coli* from cattle and swine. American Society of Agronomy Meetings, November 5-9, Minneapolis, MN.

Hartel, P. G., A. L. Funk, J. D. Summer, J. L. Hill, E. A. Frick, and M. B. Gregory. 2001. Ribotype diversity of *Escherichia coli* isolates from the Upper Chattahoochee River Watershed, Georgia. American Society for Microbiology, May 20-24, Orlando, FL.

References

Amor, K., D. E. Heinrichs, E. Frirdich, K. Ziebell, R. P. Johnson, and C. Whitfield. 2000. Distribution of core oligosaccharide types in lipopolysaccharides from *Escherichia coli*. Infect. Immun. 68: 1116-1124.

Clesceri, L. S., A. E. Greenberg, and A. D. Eaton. 1998. Standard methods for the examination of water and wastewater, 20th ed. American Public Health Association, American Water Works Association, and Water Environment Federation, Washington, DC.

Dice, L.R. 1945. Measures of the amount of ecologic association between species. Ecology 26: 297-302.

Farber, J. M. 1996. An introduction to the hows and whys of molecular typing. J. Food Protect. 59: 1091-1101.

Geldreich, E. E. 1970. Applying bacteriological parameters to recreational water quality. J. Am. Water Works Assoc. 62: 113-120.

Georgia Agricultural Statistics Service. 1999. Georgia poultry facts–1999 edition. Georgia Agricultural Statistics Service, Athens.

Georgia Department of Natural Resources. 1997. Water quality in Georgia, 1994–95. Environmental Protection Division, Atlanta.

Gregory, M. B., and E. A. Frick. 2000. Fecal-coliform bacteria concentrations in streams of the Chattahoochee River National Recreation Area, Metropolitan Atlanta, Georgia, May–October 1994 and 1995. U. S. Geological Survey Water-Resources Report 00-4139.

Grimont, F., and Grimont, P. A. D. 1986. Ribosomal ribonucleic acid gene restriction patterns as potential taxonomic tools. Ann. Inst. Pasteur/Microbiol. 137B: 165-175.

McFaddin, J. F. 1976. Biochemical tests for identification of medical bacteria. Williams & Wilkins Co., Baltimore, MD.

Myers, D.N., and F. D. Wilde. 1999. National field manual for the collection of water quality data. Biological indicators. U.S. Geological Survey Techniques of Water-Resources Investigations, Vol. 9, Chap. A7. U. S. Government Printing Office, Washington, DC.

Sambrook, J., E. F. Fritsch, and T. Maniatis. 1989. Molecular cloning: A laboratory manual. Cold Spring Harbor, NY.

Wilde, F. D., D. B. Radtke, J. Gibs, and R. T. Iwatsubo. 1999. National field manual for the collection of water-quality data. Collection of water samples. U.S. Geological Survey Techniques of Water-Resources Investigations, Vol. 9, Chap. A4. U. S. Government Printing Office, Washington, DC.

Basic Information

Title:	A Decision Support Tool for the Nile Basin
Project Number:	E-20-G67
Start Date:	5/10/2001
End Date:	11/9/2002
Research Category:	Climate and Hydrologic Processes
Focus Category:	Management and Planning, Surface Water, Hydrology
Descriptors:	Decision Support System, Reservoir Control and Operation, Water Resources Management and Planning, Flood and Drought Management, Hydropower, Remote Sensing, Agricultural Planning, International cooperation
Lead Institute:	Georgia Water Resources Institute
Principal Investigators:	Aris Peter Georgakakos

Publication

Problem and Research Objectives

The Nile River Basin is spread over ten countries covering an area of 3.1 million km^2 or approximately 10 percent of the African continent. The river discharge per unit drainage area is small, and almost all Nile water is generated from only 20 percent of the basin, while the remainder is in arid or semi-arid areas. Each region of this large watershed has distinct hydrologic features, water use requirements, and development opportunities.

This project is a collaborative effort among the Nile Basin countries, the Food and Agriculture Organization of the United Nations, and GWRI that has two primary objectives:

- Develop a comprehensive decision support tool to support the information needs of the Nile Basin stakeholders, and
- Transfer the decision support tool technology and associated knowledge base to the Nile Basin engineers and planners.

Methodology

The Nile Basin Decision Support Tool (NBDST) is composed of the following modules:

- Database: Data covering the entire basin for meteorology, hydrology, soil, terrain, land cover/land use, socio-economics, and infrastructure are to be compiled and assimilated into a user accessible database that includes GIS and presentation capabilities.
- Remote sensing of precipitation: Visible and infrared signals as received by geo-stationary satellites allow for estimation of precipitation where no ground measurements exists.
- Agricultural planning: Using detailed models of crop physiology and novel irrigation scheduling methods, a user can evaluate various scenarios of agricultural development to assess irrigation needs, food production, economic tradeoffs, etc.
- Watershed hydrology: The rainfall-streamflow response of sub-watershed in the river basin is modeled for purposes of streamflow prediction, reservoir inflows, soil moisture estimation, etc.
- River simulation and reservoir management: Optimized control processes are applied to the reservoirs in the basin for purposes of determining tradeoffs under various management scenarios. Objectives such as hydropower, irrigation, domestic water supply, and ecological integrity are assessed in their relationship vis-à-vis each other.

Technology transfer will occur through training seminars given by GWRI personnel in the Nile Basin and through extended training periods for Nile Basin personnel resident at GWRI.

Principal Findings and Significance

The NBDST project has commenced in May of 2001. Thus, there are as yet no significant results to report. Work has begun on data assimilation and software development. Dr. Aris Georgakakos, GWRI Director, has traveled to the Nile Basin to meet with professionals there to discuss project planning aspects. Project findings will be reported in future Annual Reports.

Information Transfer Program

Basic Information

Title:	Appalachicola-Chattahoochee-Flint River Basin Management Workshop
Start Date:	10/13/2000
End Date:	10/13/2000
Descriptors:	Stakeholder education, Technical methods education, River basin management
Lead Institute:	Georgia Water Resources Institute
Principal Investigators:	Aris Peter Georgakakos

Publication

The Apalachicola-Chattahoochee-Flint River Basin Management Workshop was held October 13, 2000, in Atlanta, Georgia. This one-day event was co-sponsored by GWRI and the Upper Chattahoochee Riverkeeper, a citizens interest group. The focus of the event was on relating to non-technically trained stakeholders the various technical tools being used in the ACF compact negotiation process. Speakers at the workshop included the following:

Mr. James Hathorn, U.S. Army Corps of Engineers
Mr. Steve Leitman, Northwest Florida Water Management District
Mr. Jerry Ziewitz, U.S. Fish and Wildlife Service
Dr. Aris Georgakakos, GWRI
Mr. Todd Hamill, National Weather Service

There were approximately 50 persons in attendance, and these persons came from a wide range of interests and groups. Representatives of state governments, federal agencies, private consultants, academic institutions, private companies, environmental advocates, and local interest groups were all in attendance. Positive feedback was received from the workshop attendees.

Basic Information

Title:	Lake Victoria Decision Support System (LVDSS) Advanced Training Program
Start Date:	8/1/2000
End Date:	12/31/2000
Descriptors:	Decision Support System, Reservoir Control and Operation, Water Resources Management and Planning, Flood and Drought Management, Hydropower, Remote Sensing, Agricultural Planning, International cooperation
Lead Institute:	Georgia Water Resources Institute
Principal Investigators:	Aris Peter Georgakakos

Publication

The Lake Victoria Decision Support System (LVDSS) Advanced Training Program was conducted from August 1st to December 31st, 2000. This program was sponsored by the Governments of Kenya, Tanzania, and Uganda, and the World Bank. Six professionals from the East African nations named above were in residence at Georgia Tech for advanced training in the use of the LVDSS computer software and the various methodologies behind the system. These trainees conducted various case studies of interest to their respective home countries and acquired appropriate knowledge to train others in the LVDSS usage and methodology. As a follow-up to this training program, a seminar was held in Entebbe, Uganda, in June 2001, to present the trainees' case studies and educate others about LVDSS capabilities.

The LVDSS was developed by GWRI under contract to the Food and Agriculture Organization of the United Nations in a project that took place between September 1997 and July 1999. It is a computer software system for comprehensive water resources planning and management for the Lake Victoria basin in East Africa. LVDSS database capabilities include GIS-based representations of meteorology, streamflow, soils, terrain, land cover, and socio-economic data. The application modules in the LVDSS include Remote Sensing of rainfall by satellite estimation procedures, Hydrologic Modeling, Agricultural Planning, Optimization of Hydroelectric Turbine Scheduling, and Reservoir Management.

Basic Information

Title:	GWRI Continuing Education Courses
Start Date:	3/1/2000
End Date:	2/28/2001
Descriptors:	Continuing education, Professional development, Technology transfer
Lead Institute:	Georgia Water Resources Institute
Principal Investigators:	Aris Peter Georgakakos

Publication

GWRI sponsored 3 continuing education course offerings in the past year and is continuing this important information transfer program in the current year with one course already scheduled. The courses offered include:

- Embankment Dam Design (February 2000)
- Monitoring Dam Safety (June 2000)
- Computational Fluid Dynamics for Complex Turbulent Flows (May 2001)
- Hydrologic Engineering for Dam Design (October 2001)

These courses are intended as professional development activities and do carry appropriate continuing education unit (CEU) and professional development hours (PDH) credits.

In addition to these offerings, GWRI staff are at work on development of new continuing education courses, especially for geographic information systems (GIS) applications in hydrology and water resources. A survey has been placed on the GWRI website to measure public interest in courses of this type.

USGS Summer Intern Program

Student Support

Student Support					
Category	**Section 104 Base Grant**	**Section 104 RCGP Award**	**NIWR-USGS Internship**	**Supplemental Awards**	**Total**
Undergraduate	1	5	0	0	6
Masters	0	1	0	0	1
Ph.D.	2	1	1	5	9
Post-Doc.	0	0	0	0	0
Total	3	7	1	5	16

Notable Awards and Achievements

GWRI graduate student Mr. Stephen Bourne received the 2001 ASCE Freeman Fellowship of $3000 for his Ph.D. thesis study of drought forecasting and mitigation in the Southeastern U.S. This research topic is especially timely as the region (including all of Georgia) has suffered a severe drought from approximately spring of 1998 to the present.

Publications from Prior Projects

1. Weber, D., 2000, "Relative Contribution of Sediment from Upland and Channel Erosion," M.S. Thesis, School of Civil and Environmental Engineering, Georgia Institute of Technology.
2. Brumbelow, K., and A. Georgakakos. 2001. "An Assessment of Irrigation Needs and Crop Yield for the United States under Potential Climate Changes." Journal of Geophysical Research - Atmospheres. in press.